Available online at www.sciencedirect.com
ScienceDirect
Gondwana Research 11 (2007) 92–108
www.elsevier.com/locate/gr

Geochemistry and geochronology of the Neoproterozoic Pan-African Transcaucasian Massif (Republic of Georgia) and implications for island arc evolution of the late Precambrian Arabian–Nubian Shield

Guram S. Zakariadze [a], Yildirim Dilek [b,*], S.A. Adamia [c], R.E. Oberhänsli [d], S.F. Karpenko [a], B.A. Bazylev [a], N. Solov'eva [a]

[a] *Vernadsky Institute of Geochemistry and Analytical Chemistry, Russian Academy of Sciences, Moscow 119991, Russia*
[b] *Department of Geology, Miami University, Oxford OH 45, USA*
[c] *Dzhavakhishvili Tbilisi State University, pr. Chavchavadze 1, Tbilisi, 380028 Georgia*
[d] *Institut fur Geowissenschaften, Universitat Potsdam, Potsdam, D-14415 Germany*

Received 27 April 2006; received in revised form 13 May 2006; accepted 15 May 2006
Available online 7 September 2006

Abstract

The Transcaucasian Massif (TCM) in the Republic of Georgia includes Neoproterozoic–Early Cambrian ophiolites and magmatic arc assemblages that are reminiscent of the coeval island arc terranes in the Arabian–Nubian Shield (ANS) and provides essential evidence for Pan-African crustal evolution in Western Gondwana. The metabasite–plagiogneiss–migmatite association in the Oldest Basement Unit (OBU) of TCM represents a Neoproterozoic oceanic lithosphere intruded by gabbro–diorite–quartz diorite plutons of the Gray Granite Basement Complex (GGBC) that constitute the plutonic foundation of an island arc terrane. The Tectonic Mélange Zone (TMZ) within the Middle-Late Carboniferous Microcline Granite Basement Complex includes thrust sheets composed of various lithologies derived from this arc-ophiolite assemblage. The serpentinized peridotites in the OBU and the TMZ have geochemical features and primary spinel composition (0.35) typical of mid-ocean ridge (MOR)-type, cpx-bearing spinel harzburgites. The metabasic rocks from these two tectonic units are characterized by low-K, moderate-to high-Ti, olivine-hypersthene-normative, tholeiitic basalts representing N-MORB to transitional to E-MORB series. The analyzed peridotites and volcanic rocks display a typical melt-residua genetic relationship of MOR-type oceanic lithosphere. The whole-rock Sm–Nd isotopic data from these metabasic rocks define a regression line corresponding to a maximum age limit of 804±100 Ma and εNd_{int}=7.37±0.55. Mafic to intermediate plutonic rocks of GGBC show tholeiitic to calc-alkaline evolutionary trends with LILE and LREE enrichment patterns, Y and HREE depletion, and moderately negative anomalies of Ta, Nb, and Ti, characteristic of suprasubduction zone originated magmas. U–Pb zircon dates, Rb–Sr whole-rock isochron, and Sm–Nd mineral isochron ages of these plutonic rocks range between ~750 Ma and 540 Ma, constraining the timing of island arc construction as the Neoproterozoic–Early Cambrian. The Nd and Sr isotopic ratios and the model and emplacement ages of massive quartz diorites in GGBC suggest that pre-Pan African continental crust was involved in the evolution of the island arc terrane. This in turn indicates that the ANS may not be made entirely of juvenile continental crust of Neoproterozoic age. Following its separation from ANS in the Early Paleozoic, TCM underwent a period of extensive crustal growth during 330–280 Ma through the emplacement of microcline granite plutons as part of a magmatic arc system above a Paleo-Tethyan subduction zone dipping beneath the southern margin of Eurasia. TCM and other peri-Gondwanan terranes exposed in a series of basement culminations within the Alpine orogenic belt provide essential information on the Pan-African history of Gondwana and the rift-drift stages of the tectonic evolution of Paleo-Tethys as a back-arc basin between Gondwana and Eurasia.

Keywords: Transcaucasian massif; Neoproterozoic ophiolites; Arabian–Nubian Shield; Pan-African crust; Precambrian island arc evolution; Paleo-Tethys; Paleozoic Eurasia

1. Introduction

The Pan-African evolution of Gondwana during the Neoproterozoic–Early Cambrian signifies an important period in the

* Corresponding author. Tel.: +1 513 529 2212; fax: +1 513 529 1542.
E-mail address: dileky@muohio.edu (Y. Dilek).

1342-937X/$ - see front matter © 2006 International Association for Gondwana Research. Published by Elsevier B.V. All rights reserved.
doi:10.1016/j.gr.2006.05.012

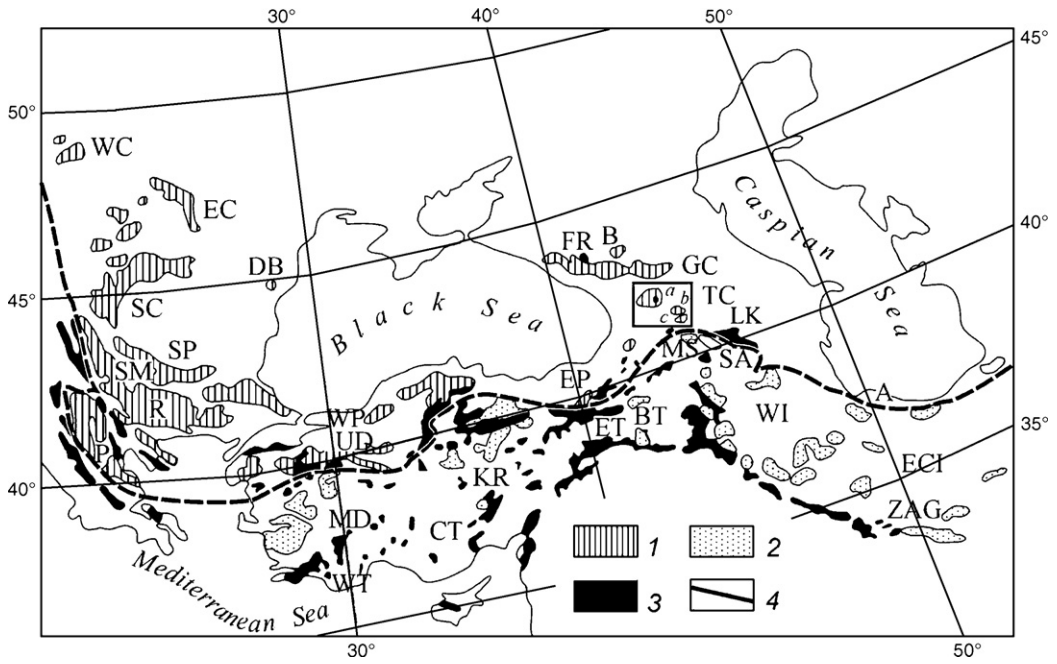

Fig. 1. Simplified geological map of the Late Precambrian crystalline basement culminations and the Mesozoic suture zones in the Eastern Mediterranean region. 1—Hercynian granite-metamorphic basement; 2—Precambrian granite-metamorphic basement; 3—Mesozoic ophiolites and mélange zones; 4—Paleo-Tethyan suture zone (dashed). Abbreviations: WC, EC, SC — Western, Eastern, and Southern Carpathians; DB—Dobrudja; SP – Stara Planina; SM—Serbo-Macedonian massif; R — Rhodope massif; P — Pelagonian massif; WP, EP — Western and Eastern Pontides (respectively); MD — Menderes massif; KR — Kirsehir massif; WT, CT, ET — Western, Central and Eastern Taurides (respectively); UD — Uludag massif; BT — Bitlis massif; GC — Main Range of the Great Caucasus; TC — Transcaucasian massif (a—Dzirula; b—Khrami; c—Lokhi salients); SA—Sevano–Akera zone; WI, ECI — Western Iran and East-Central Iran; A—Alborz; ZAG—Zagros. Box depicts the study area.

Earth's geological record because of the rapid and extensive growth of continental crust through accretion of ophiolites and volcanic arc terranes (Stern, 1994, 2004, and references therein). It is commonly believed that the beginning of the Neoproterozoic era also marks a major change in Earth's evolution with the onset of modern plate tectonic systems (Stern, 2004). Therefore, the mode and nature of tectonic, magmatic, and metamorphic processes during the Pan-African evolution of Gondwana need to be carefully documented in order to better understand how plate tectonic systems worked in this critical time window between the Early Precambrian and the beginning of the Phanerozoic. However, it is difficult to discern the complete tectonic history of Gondwana and to test the competing hypotheses for its evolution because younger events obliterated much of the geological evidence for the Pan-African evolution. Some of these events included lithospheric-scale deformation associated with dismantling of Rodinia around 1000 Ma and subsequent opening of various ocean basins (e.g., Rheic, Proto-Tethys, Paleo-Tethys), plate collisions, collision-driven escape tectonics, and extensive magmatism, metamorphism, and deformation associated with active margin evolution.

Fortunately, the missing Pan-African links between Late Precambrian crustal evolution and Early Phanerozoic tectonics can be found in the peri-Gondwanan terranes, now exposed in a series of basement culminations within the Alpine orogenic belt. These Neoproterozoic–Cambrian crustal fragments, which all appear to have been derived from Afro-Arabia occur in tectonically exhumed regions in the Carpathians, Balkanides, Dinaride-Hellenides, Thrace, Pontides, and Caucasus. In contrast, the Bohemian, Armorican, Cadomian, and Iberian massifs in Western Europe represent the peri-Gondwanan terranes with genetic links to the West African part of Gondwana and may also have had spatial connections to Amazonia and Laurentia during the Neoproterozoic (Murphy et al., 2004). Therefore, systematic field, geochemical, and geochronological studies of the Neoproterozoic–Cambrian ophiolites and arc complexes in the peri-Gondwanan fragments in the eastern Mediterranean region should provide new insights into the mantle chemistry and dynamics, mid-ocean ridge and subduction zone processes, and crustal evolution during the Late Precambrian buildup of the ANS.

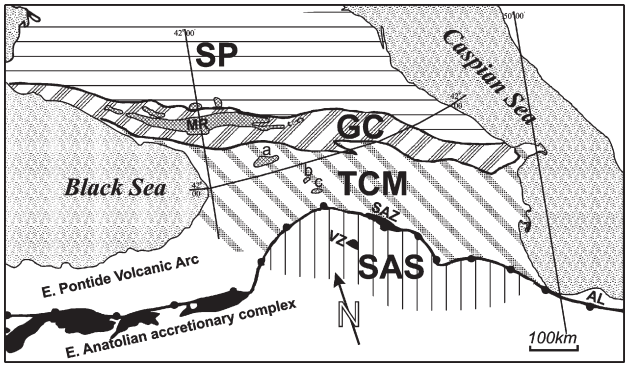

Fig. 2. Major Structural Units of the Caucasus. SP — Scytian Platform; GC — Great Caucasus (MR — Main Range); TCM — Transcaucasian Massif (a—Dzirula, b—Khrami, c—Loki salients); SAS — South Armenian Subplatform. SAZ – Sevano–Akera ophiolite zone; VZ — Vedi ophiolite zone; AL — Alborz Mountains. The line with black dots indicates the Eastern Pontide–Lesser Caucasus paleo-oceanic suture zone and corresponds to the southern border of the Eastern Pontide and Caucasus Hercynides.

In this paper, we present new geochemical, isotopic, and geochronological data from the Neoproterozoic–Cambrian ophiolitic and island arc rocks in the TCM (Fig. 1), documenting its Pan-African origin and its genetic relationship with the ANS. These new data and interpretations suggest that the Neoproterozoic–Cambrian island arc evolution in the ANS was reminiscent of ensimatic arc construction within subduction zone environments fringing continental masses, such as in the Jurassic western U.S. Cordillera (Dilek et al., 1991) and in the Late Cenozoic Lesser Antilles (Davidson, 1986; White and Dupre, 1986). We discuss in the last part of the paper the tectonic evolution of the TCM within the Gondwana and Eurasia realms and the tectonic implications of this complex evolutionary pattern for rapid continental growth during the Neoproterozoic and Paleozoic.

2. Geology of the Transcaucasian Massif

The Transcaucasian Massif (TCM) is one of the major tectonic units in the Caucasus and is situated between the Southern Slope Zone of the Great Caucasus in the north and the Lesser Caucasus suture zone in the south (Fig. 2). It consists of a crystalline basement, exposed in the Dzirula, Khrami, and Loki salients (from north to south, respectively, Fig. 3), that is overlain by a non-metamorphosed and moderately folded, nearly 10-km-thick Upper Triassic through Cenozoic volcano-sedimentary cover. The basement succession of the TCM consists mainly of the following units: (1) Late Proterozoic–Early Paleozoic *Oldest Basement Unit*, (2) Neoproterozoic–Cambrian *Gray Granite Basement Complex*, (3) Middle-Late Carboniferous *Microcline Granite Basement Complex*, and (4) Late Proterozoic–Early Paleozoic Tectonic Mélange Zone. The contact relations among the first three meta-igneous units are commonly intrusive, although extensively modified by superimposed metamorphic events. The rock units in the Tectonic Mélange Zone are in fault contact with the Carboniferous Microcline Granite Basement Complex and include slices of Cambrian–Late Devonian serpentinite, amphibolite, phyllite, and Middle-Late Paleozoic microcline granite and high-silica volcanic rocks (Adamia, 1984; Zakariadze et al., 1998; Gamkrelidze and Shengelia, 1999; Gamkrelidze et al., 1999).

2.1. Oldest basement unit (Late Proterozoic–Early Paleozoic)

This unit consists mainly of biotite-gneiss, plagiogneiss, amphibolite, schist (plagioclase-amphibole, actinolite-chlorite-albite, chloritoid, chloritoid-chlorite-phengite, andalusite-muscovite, and cordierite) and graphite quartzite, and can be subdivided into *metabasic* and *metasedimentary* subunits. These high-grade metamorphic rocks occur either in allochthonous thrust sheets or as xenoliths in younger gabbroic, dioritic and quartz dioritic intrusions. The *metabasic subunit* includes massive and banded amphibolite, garnet amphibolite, metadiabase, and subordinate hypabyssal bodies of metagabbro, diabase, and cpx-and amphibole-metagabbro. Gneissic basic lava-breccias, metatuff, and metagreywacke are also present in the metabasic subunit. The mineral association of the metabasic series varies from greenschist facies assemblages (actinolite-chlorite-albite) and epidote-amphibolites, up to plagioclase-and locally garnet-plagioclase-amphibolites (Zakariadze et al., 1998). The Oldest Basement Unit exposed in the Loki salient includes metamorphosed sheeted dikes and pillow lavas, suggesting that it may represent a meta-ophiolite (Gamkrelidze et al., 1999). The subordinate *metasedimentary subunit* consists of various types of schist (plagioclase-amphibole, actinolite-chlorite-albite, chloritoid, chloritoid-chlorite-phengite, andalusite-muscovite, cordierite), biotite-gneiss, plagioclase-gneiss, plagioclase migmatite, minor amphibolite, graphitic quartzite, and scarce marble. These metasedimentary rocks locally alternate with metavolcanic layers (Shengelia et al., 1988; Adamia et al., 1990).

Pressure–temperature estimates of the prograde metamorphism experienced by the protoliths of the Old Basement Unit suggest andalusite-sillimanite pressure conditions in a temperature interval of biotite-to sillimanite-muscovite-potassium feldspar zone (sillimanite-potassium feldspar-garnet). Mineral associations of high-silica igneous and metasedimentary rocks in this temperature interval vary from biotite-muscovite-chlorite and chloritoid-schists (greenschist facies) through andalusite-biotite-muscovite-cordierite gneisses to sillimanite-cordierite-muscovite-potassium feldspar gneisses and migmatites, corresponding to the medium amphibolite facies conditions (<650 °C; Korikovsky, 1979; Shengelia and Okrostsvaridze, 1998).

2.2. Gray granite basement complex (Neoproterozoic–Cambrian)

This unit includes mafic to intermediate intrusions emplaced at various structural levels in the Oldest Basement Unit (Fig. 3). Mafic intrusions consist of dikes and small stocks of massive, aphyric, and/or plagioclase phyric diabase, gabbro-diabase, and medium-grained olivine-bearing pyroxene-and amphibole-gabbro (up to 80–800 m thick). Intrusions with intermediate compositions consist of coarse-grained diorite and quartz diorite and include two sub-types: (1) diorite and quartz diorite gneiss, and (2) massive diorite, quartz diorite, and minor low-K granite. Both sub-types have similar mineralogical compositions (plagioclase-amphibole-biotite-potassium feldspar±quartz); however, the textural and mineralogical features observed in the quartz diorite gneiss point to the physical conditions of metamorphism and deformation typical of the biotite-sillimanite-muscovite zone. Diorite and quartz diorite intrusions include numerous xenoliths of the Old Basement Unit rocks.

2.3. Tectonic mélange zone (Late Proterozoic–Early Paleozoic)

The Tectonic Mélange occurs in a NE–SW trending shear zone hosted within the Middle–Late Carboniferous microcline granite rocks of the Microcline Granite Basement Complex in the eastern part of the Dzirula salient (Fig. 3); this 1.5 km-wide mélange belt is also known locally as the *Chorchana–Utslevi Zone* (CHUZ). The tectonic mélange is unconformably overlain by the Upper Triassic–Upper Jurassic sedimentary cover of the TCM (Adamia, 1984; Svanidze et al., 2000) and includes thrust sheets composed of metabasite and serpentinite, phyllite, high-silica volcanic rocks, and a Late Carboniferous microcline granite

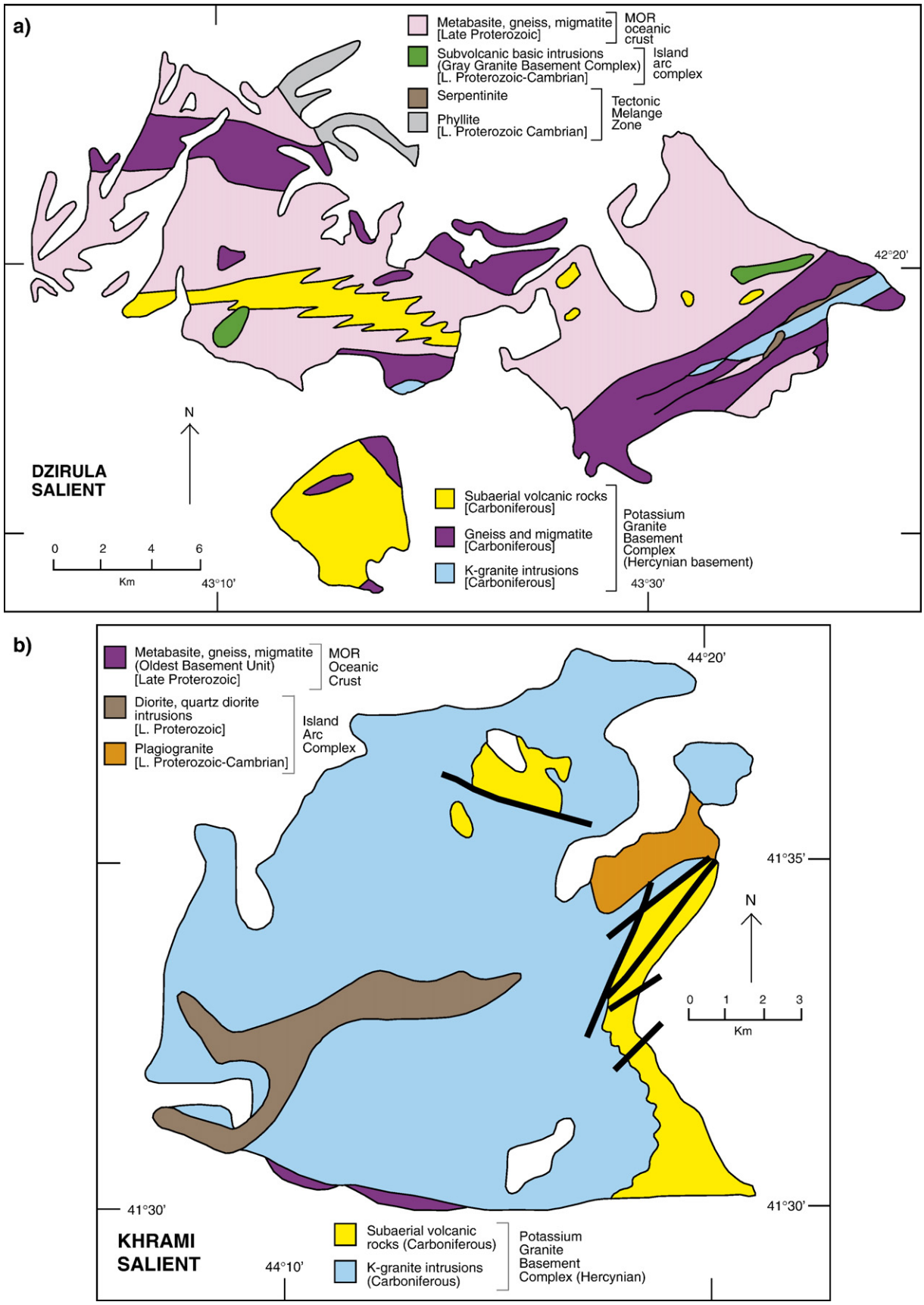

Fig. 3. Simplified geological maps of the major salients (basement culminations) in the Transcaucasian massif.

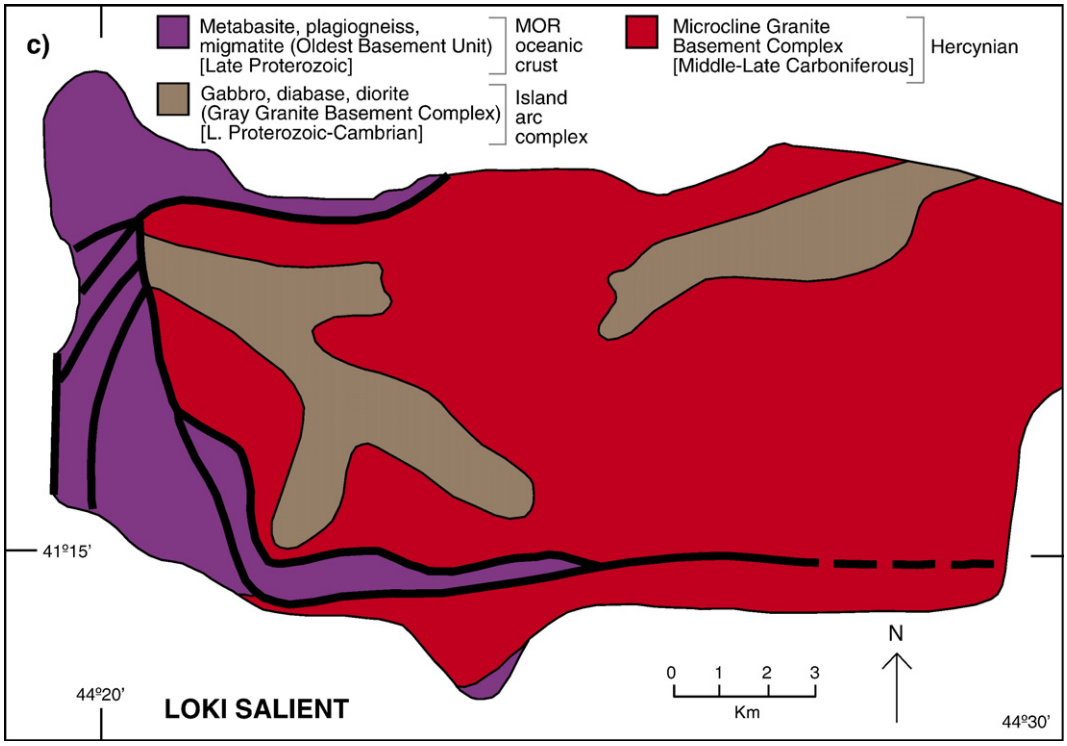

Fig. 3 (*continued*).

(Adamia, 1984; Abesadze et al., 1989). Metabasic rocks in this mélange consist of massive and banded amphibolites, mylonitized amphibolite, metagabbro, metadiabase, and metabasic tuff. Phyllitic rocks that show a wide age interval from the Cambrian to the Late Devonian (Abesadze et al., 1980) correspond to metasediments represented by aluminous pelitic, silty, and psammitic rocks with interbedded limestone that were metamorphosed at greenschist-facies conditions. The mafic–ultramafic association of the mélange zone has been interpreted as a dismembered Late Proterozoic–Early Paleozoic meta-ophiolite, and the phyllite slices as fragments of the sedimentary cover of this ophiolitic basement (Adamia and Shavishvili, 1979; Gamkrelidze et al., 1981; Adamia, 1984; Zakariadze et al., 1998).

2.4. Microcline granite basement complex (Middle-Late Carboniferous)

The Middle-Late Carboniferous Microc-line Granite Basement Complex intrudes the Oldest Basement Unit and the Gray Granite Basement Unit and constitutes more than 50% of the crystalline basement in the TCM. We have distinguished two major types of rock associations in the Microcline Granite Basement Complex: a plutonic microcline granite suite and a high-silica, shallow-water to subaerial volcano-sedimentary sequence. The microcline granite suite is areally more extensive and consists of potassium-rich microcline-gneiss-migmatite and microcline-granite. It includes two main sub-groups: one sub-group is a result of extensive migmatization of both the Oldest Basement Unit and the Gray Granite Basement Complex and is composed of heterogeneous microcline-biotite gneiss and migmatite rocks containing inclusions of older series. Fragments of the mafic rocks are the most common inclusion types. The other sub-group encompasses massive, uniform microcline granite, muscovite granite, leucogranite, aplitic dikes (up to several meters thick), and stocks (up to 200–300 m in diameter) and veins of muscovite granite and pegmatite.

A shallow-water to subaerial high-silica volcano-sedimentary sequence is well exposed in the Dzirula and Khrami salients. This volcano-sedimentary subunit is Visean–Bashkirian (~350–320 Ma) in age and 1200–1300 m in thickness, consisting mainly of lava flows, lava-breccias, and rhyolitic pyroclastic deposits, alternating with shallow-water, siliceous, terrigeneous, and subordinate carbonaceous sedimentary rocks.

3. Geochemistry

3.1. Analytical techniques

The analytical work was carried out at the Vernadsky Institute of Geochemistry and Analytical Chemistry in the Academy of Sciences of Russia, Moscow. The major elements were determined by XRF, and LILE and HFSE by ICP (analysts L.A. Roschina, T.V. Romasheva, and L.N. Bannikch). REE, Th, Ta, Hf were determined by INAA methods (analysts G.M. Kolesov—basic rocks and S.M. Lyapunov—peridotites). Replicate analyses for major elements, LILE, and HFSE for some key samples were carried out by XRF at the University of Mainz, Institut fuer Geowissenschaften, Germany (analyst M. Koziol). The analytical results are listed in Tables 1, 2, 3, and 4.

The technique for our Sm–Nd isotopic analyses has been described in Wasserburg et al. (1981) and Karpenko et al. (1984). Whole rock samples weighing about 50 g and having no visible traces of any alterations were crushed in steel mortars and then pulverized in agate mortars. Mineral fractions for isochrons were separated from crushed samples (0.5 mm size fraction) using standard procedures involving electromagnetic and heavy liquids separation. Final purification of the mineral fractions was done by hand under binocular microscope. Small portions of the samples (from 50–100 mg in weight) were dissolved in Teflon bombs at high temperature (180 °C) until dissolution was complete. An aliquot of mixed ^{147}Sm–^{150}Nd trace solution was then added to each of the samples. Separation of the REE fraction was made using standard ion-exchange column chromatography on BioRad AG 50X8 cation resin. Nd was separated from Sm on a cation exchange resin BioRad 50X4 with α-methyllatic acid as an eluent. This technique of Nd and Sm separation has important advantage allowing us to obtain Nd practically free of Ce; the intensity of ion current from the most abundant Ce isotope (^{140}Ce) was usually less than one thousandth of that from ^{145}Nd. This in turn allows us to use $^{150}Nd/^{142}Nd$ ratio for normalization of raw mass-spectrometric data. In our case, this ratio is assumed to equal 0.209627. According to the applied analytical procedures, further treatment of the obtained Nd isotopic data should be done using parameters: $^{143}Nd/^{144}Nd_{chur}(0)=0.511947$; $^{147}Sm/^{144}Nd_{chur}(0)=0.1967$; $\varepsilon_{sm}=0.00654$ Ga-1.

Mass-spectrometric measurements were done on Cameca TSN 206 SA mass-spectrometer. Samples of Nd and Sm were loaded on a triple-filament (Re, W) W evaporator ion source, and ion currents from metal ions were measured. The precision of the data was controlled from the regular measurements of our inter-laboratory isotope standard calibrated against the Ames Nd metal. At the same time, the precision could be evaluated from the constancy of non-radiogenic isotope ratios, which were measured in every run. Isochrons were calculated using Ludwig's Izoplot program. The precision of the $^{147}Sm/^{144}Nd$ ratio was estimated as ±0.3% for all the samples. Total blanks (not more than several tens of picograms) were practically negligible as the quantity of Nd, separated from the samples, was several hundreds of nanograms. The results are shown in Tables 4 and 5.

3.2. Ultrabasic–basic association

Metabasic rocks in the TCM are commonly found as amphibolites in the Oldest Basement Unit and are spatially associated with serpentinites in the Tectonic Mélange Zone. Ultrabasic rocks in the Tectonic Mélange Zone generally occur as lens-like bodies (less than 1 km^2) within a suite of schist rocks and along the contact of this suite with various gabbro-diorite intrusions, and locally as xenoliths in these intrusions. These ultrabasic rocks are represented by serpentinites, which show massive or coarse-banded textures. Secondary amphibole, talc, and carbonate development is widespread in these rocks, in which bastite after pyroxene minerals constitute nearly 30% of the rock-forming minerals. Spinel minerals form as relatively large irregularly shaped grains in serpentinized olivine and as small euhedral grains along the periphery of bastites. They are mostly opaque and are represented by secondary (metamorphic) chrome spinel. Relics of the primary brown spinels are preserved only in rare large spinel grains. The composition of the primary spinel ($Cr/(Cr+Al)=0.349$; $Mg/(Mg+Fe^{2+})=0.712$; Table 1) corresponds well to the compositions of abyssal spinel-peridotites (Dick and Bullen, 1984), although its titanium content (0.15 wt. % TiO_2) and iron oxidation degree ($Fe^{3+}/(Cr+Al+Fe^{3+})=0.036$ are somewhat elevated. The bulk-rock compositions of the ultramafic rocks (Table 1) were affected by metamorphism, serpentinization, and carbonatization, disturbing their calcium contents. However, their aluminum, titanium, and chromium contents suggest their protolith as clinopyroxene-bearing spinel harzburgite. The high nickel contents, the high Ni/Co ratio, and the low vanadium contents are consistent with this conclusion. The data on the bulk-rock REE contents (Table 1) demonstrate a regular depletion pattern only for HREE (from 0.40 to 0.36 of chondritic contents), whereas the MREE and LREE patterns show regular enrichment. It is unclear whether this enrichment was a primary rock feature or was a result of metamorphism. Nevertheless, all the chemical features of these serpentinized peridotites, including their LREE enrichment patterns, fall within the ranges known for abyssal Cpx-bearing spinel

Table 1
Whole rock and spinel compositions for the Dzirula salient peridotites in the Transcaucasian Massif

Sample no	D1-84	D51-84	D65-84	D66-84	STD	D1-84
	WR	WR	WR	WR	WR	Spl*
SiO_2	38.67	39.24	39.88	38.99	0.19	0.08
TiO_2	0.026	0.027	0.021	0.016	0.006	0.15
Al_2O_3	1.15	1.61	1.15	0.88	0.02	37.36
FeO	6.11	6.45	7.26	7.01	0.04	15.15
MnO	0.116	0.125	0.109	0.107	0.002	0.16
MgO	35.64	37.39	36.32	37.53	0.50	16.80
CaO	1.51	0.11	0.15	0.72	0.01	
Na_2O		0.08	0.08	0.06	0.03	
K_2O		0.02	0.04	0.02	0.01	
Cr_2O_3	0.389	0.534	0.337	0.359	0.002	29.90
NiO						0.19
P_2O_5	0.032	0.009	0.016	0.008	0.004	
LOI	15.80	14.58	14.81	14.74		
Total	99.44	100.17	100.18	100.43		99.79
Cu		4	9	7	2	
Ni		2068	2159	2099	66	
Sr		3	8	5	2	
Ti		138	n.d.	78	11	
V		43	35	28	4	
Zn		71	58	53	5	
Co		86	92	94	8	
Sc		15	n.d.	5	2	
Y		2	<4	1	1	
La			0.94			
Ce			1.5			
Nd			0.54			
Sm			0.11			
Eu			0.027			
Tb			0.013			
Yb			0.058			
Lu			0.0097			

(Oxides in wt.%, trace elements and REE in ppm).
* Analysis from Zakariadze et al., 1998.

harzburgites (Niu, 2004). Thus, we interpret them as MOR-type, clinopyroxene-bearing spinel harzburgites, representing restites after extraction of tholeiitic basaltic melts (Zakariadze et al., 1998). However, their possible origin in a back-arc spreading center cannot be ruled out.

The metabasic rocks in the Oldest Basement Unit and the Tectonic Mélange Zone (Table 2) consist mainly of low-potassium ($K_2O<1$ wt.%), moderate-to high-titanium (1.5–3.1 wt.% TiO_2), olivine-hypersthene-normative, differentiated (Mg#=0.69–0.53) tholeiitic basalts. We have distinguished two geochemical subgroups of these basalts as N-type and transitional to E-type MORB (Fig. 4 a, b). The N-MORB basalts, which are sampled in the Tectonic Mélange Zone of the Dzirula salient, are characterized by their moderate titanium (TiO_2= 1.48±0.34 wt.%) low REE (41±12 ppm) contents, and flat or slightly LREE-depleted patterns [$(La/Sm)_n$=0.82±0.32; $(La/Yb)_n$=0.76±0.38; $(Sm/Yb)_n$=0.90±0.22; $(Yb)_{morb}$=0.99±0.23]. The transitional to E-MORB basalts, which delineate a high-Ti subgroup (TiO_2=2.32±0.75 wt.%), occur both in the Tectonic Mélange Zone and in the Oldest Basement Unit and are relatively enriched in REE (97±16 ppm), LREE [$(La/Sm)_n$=2.7±0.04; $(La/Yb)_n$=5.25±1.52; $(Sm/Yb)_n$=1.94± 0.54; $(Yb)_{morb}$=0.74± 0.15], as well as in Th and Zr. These basalts have higher Th/La=0.19±0.12, Th/Sm=0.78±0.49, Th/Yb=1.60±1.23, and Zr/Y=4.03±1.09 ratios in comparison to the N-MORB basalts.

3.3. Gray granite basement complex

The diabase and gabbro-diabase intrusions in the Oldest Basement Unit that constitute the mafic component of the Gray Granite Basement Complex have the compositions of fractionated olivine-hypersthene, and quartz-normative low-titanium basalt (49.26±1.73 wt.% SiO_2; 0.66±0.31 wt.% TiO_2), basaltic andesite (53.10±0.37 wt.% SiO_2), and andesite (57.27± 1.48 wt.% SiO_2) and show transitional chemical features between tholeiitic and calc-alkaline series (Table 3; Fig. 4c). The rocks with basaltic compositions predominate and display wide fractionation limits as suggested by their Mg number (Mg#=0.77–0.43). The whole intrusive unit is LILE-enriched (Rb/Y=2.34+0.73) and LREE [$(La/Sm)_n$=2.20±0.50; $(La/Yb)_n$=5.53±1.11], relatively depleted in Y and HREE [$(Yb)_{MORB}$=0.70±0.17], and shows moderately negative geochemical anomalies of tantalum (Ta/Ta*=0.42±0.06), niobium (Nb/Nb*=0.45) and titanium (Ti/Ti*=0.86±0.2). Slight Eu anomalies (Eu/Eu*=1.07±0.29) and high Th/Ta ratios (4.85± 1.05) are also common in these mafic rocks.

Table 2
Major and trace element abundances of metabasics from the Tectonic Melange Zone and the oldest Basement Unit of the Transcancasian Massif

Sample no	47-84	49-84	50-84	57-84	58-84	59-84	71-84	Mash-1	Mo-2
SiO_2	48.38	47.46	49.4	48.3	49.48	49.98	49.94	47.22	47.94
TiO_2	1.78	1.03	0.96	1.63	1.5	1.64	1.79	1.7	2.99
Al_2O_3	12.47	16.07	15.25	13.98	15.48	14.6	18.79	15.45	14.66
FeO	12.03	10.12	9.53	10.61	9.14	10.12	8.56	10.71	13.87
MnO	0.21	0.19	0.17	0.19	0.18	0.2	0.16	0.24	0.19
MgO	7.5	7.97	7.69	7.54	7.63	7.31	6.52	9.18	4.33
CaO	9.72	8.48	8.44	9.68	10.21	9.16	10.86	8.65	12.7
Na_2O	2.99	2.67	2.73	3.13	2.51	3.35	2.06	2.87	0.72
K_2O	0.44	0.69	1.18	0.48	0.72	0.62	1.13	0.2	0.95
P_2O_5	0.21	0.13	0.11	0.18	0.19	0.2	0.3	0.19	0.37
LOI	3.72	4.46	3.67	4.22	2	2.02	0.52	2.74	1.45
Total	99.59	99.33	99.13	99.94	99.04	99.2	100.6	99.15	99.78
Rb	10	14	22	17	32	28	22	7	430
Ba	102	–	–	–	–	–	–	31	635
Sr	108	495	490	230	202	210	328	306	430
Zr	91	52	34	100	80	70	150	138	65
Y	39	24	30	35	50	64	51	27	–
Nb	5	1	7	8.4	9.3	7.9	8.2	21	–
Th	0.35	0.1	0.2	0.66	0.45	0.27	5.1	1	1.49
Ta	0.32	0.11	0.2	0.2	–	0.36	–	2.5	1.31
Hf	2.03	1.05	0.41	3.13	2	2.83	1.5	0	4.73
La	3.2	1.8	0.88	3.98	5.34	4.27	17	14	21.1
Ce	9	5.1	2.77	10.8	12	10.3	35	27	41.4
Pr	1.4	0.87	0.53	1.6	1.7	1.45	4	3	5.00
Nd	8.3	4.7	3.3	7.9	8.9	6.9	15	12	20.2
Sm	3.27	1.93	1.34	2.76	3.23	2.14	4	3.4	5.31
Eu	1.23	0.71	0.73	1.17	1.25	1.24	1.3	0.75	2.27
Gd	4.9	2.84	3	6.1	4.3	4.4	5	4.7	6.72
Tb	0.86	0.54	0.52	0.98	0.7	0.69	0.7	0.75	1.09
Dy	5.8	3.4	3.2	6	4.7	4.5	4.2	4.7	6.48
Ho	1.3	0.8	0.77	1.37	1	1.09	0.9	1.1	1.49
Er	4.1	2.4	2.4	4	3	3.3	2.5	3.1	4.32
Tm	0.65	0.38	0.4	0.59	0.48	0.53	0.38	0.47	0.63
Yb	4.13	2.3	2.27	3.48	2.8	3.21	1.8	2.7	3.78
Lu	0.7	0.39	0.42	0.57	0.46	0.54	0.37	0.45	0.61

Table 3
Major and trace element abundances of subvolcanic basic intrusions of the oldest Gray Granite Basement Complex

Sample	73-84	4-87	GZ-2	LG-2	LG-4
SiO_2	51.60	53.10	45.07	50.80	49.72
TiO_2	0.97	0.94	1.90	1.77	1.90
Al_2O_3	16.50	20.30	17.17	16.09	16.34
FeO	7.91	6.00	15.42	9.93	9.95
MnO	0.15	0.11	0.12	0.21	0.25
MgO	6.52	4.00	6.56	4.44	5.55
CaO	9.63	8.30	9.84	9.48	8.94
Na_2O	2.29	1.60	0.98	2.85	1.24
K_2O	1.18	1.90	1.05	0.03	1.14
P_2O_5	0.24	0.22	0.07	0.25	0.24
LOI	1.65	3.25	1.90	4.18	4.33
Total	99.05	99.72	99.85	99.77	99.35
Rb	32	64	16.3	–	46.4
Ba	–	565	405	600	590
Sr	212.0	307.0	45.0	795.0	485.0
Zr	80	120	340	84	320
Y	21.0	25.0	20.3	27.7	24.0
Nb	8.20	7.00	–	–	–
Th	1.75	2.00	1.43	5.29	4.18
Ta	0.31	0.49	0.43	0.66	0.47
Hf	1.70	2.60	4.64	4.99	3.64
La	7.42	17.50	23.20	14.70	18.20
Ce	16.40	34.00	49.10	33.80	34.70
Pr	2.10	4.10	6.08	4.52	3.90
Nd	9.60	16.40	26.00	21.30	14.90
Sm	2.57	4.20	7.38	6.40	3.89
Eu	1.03	1.20	1.48	1.73	1.97
Gd	3.00	4.50	8.30	8.20	4.95
Tb	0.45	0.72	1.17	1.21	0.77
Dy	2.60	4.20	6.30	7.00	4.68
Ho	0.56	0.88	1.29	1.49	10.9
Er	1.40	2.50	3.34	4.04	3.01
Tm	0.20	0.36	0.46	0.56	0.46
Yb	1.01	2.00	2.20	3.00	2.60
Lu	0.18	0.35	0.34	0.48	0.44

The coarse-grained diorite and quartz diorite intrusive bodies within the Gray Granite Basement Complex are composed of gabbro (14%), diorite (40%), quartz diorite (33%) and granite (13%), and display transitional chemical features from tholeiitic to calc-alkaline series (Table 4; Fig. 4d). Pronounced enrichment in Th, distinct negative anomalies of tantalum, niobium, and titanium ($Ta/Ta^*=0.2\pm0.09$; $Nb/Nb^*=0.25\pm0.10$ and $Ti/Ti^*=0.57\pm0.24$), and prominent variations of Eu anomalies ($Eu/Eu^*=5.75-0.31$) are characteristic features of these dioritic-quartz dioritic rocks. They also show a moderate enrichment in LREE [$(La/Yb)_{pm}=7.68\pm2.57$], flat HREE patterns [$(Tb/Yb)_{pm}=1.73\pm0.45$], and low contents of Y and Yb [$(Yb)_{MORB}=0.57\pm0.22$]. All these geochemical features along with characteristic Th/Yb–Ta/Yb relations (see Fig. 7, for example) indicate a suprasubduction origin of the magmatic rocks of the Gray Granite Basement Complex.

The geochemical data from the Oldest Basement Unit (including the metasedimentary successions) predating the Gray Granite Basement Complex are limited. The available major-element data from the volcanic interlayers in this succession suggest that these rocks are made of low-titanium basalt (48.5± 2.3 wt.% SiO_2; 0.48±0.16 wt.% TiO_2), andesite (57.8±2.2 wt.% SiO_2), dacite (65.90±0.72 wt.% SiO_2), and rhyolite (72.3± 0.51 wt.% SiO_2) that are transitional between tholeiitic and calc-alkaline series.

4. Geochronology

The geochronological and biostratigraphic data available from the Neoproterozoic–Cambrian basement units of the TCM are summarized in Table 8. We present our new Sm–Nd isochron data in Tables 5 6 and 7. We defined the age of the basic–ultrabasic associations in the TCM based on Nd isotope variations for the metabasic series in the Tectonic Mélange Zone (Table 5; Fig. 4a). These rocks show significant variations of the Sm/Nd ratio (0.41–0.27) despite their narrow variation ranges for major elements ($Mg\#=0.58\pm0.01$). The whole-rock Sm–Nd isotopic data from the amphibolites in the Tectonic Mélange Zone define a regression line corresponding to the age of 804± 100 Ma and $\varepsilon Nd_{int}=7.37\pm0.55$ (see Fig. 5a).

To evaluate the source of this isotopic variation, we have made the following three assumptions regarding the possible relationship between the isotopic and trace element data from the basic–ultrabasic series we have analyzed. First, because both basic and ultrabasic rocks in the Tectonic Mélange Zone have MORB affinities with narrow major-element variation limits, we interpret these rocks as part of the same ancient oceanic lithosphere, which was subsequently dismembered during obduction. This ancient oceanic lithosphere and the meta-ophiolitic rocks in the Old Basement Unit are likely to have constituted the ancient mafic foundation of the TCM. Second, because MORB lavas with varying degrees of REE fractionation are common occurrences along the modern mid-ocean ridge segments, the inferred REE fractionation of the TCM basalts is interpreted to have occurred in a single magmatic event. Third, the magmatic event that produced the MORB crust in the Oldest Basement Unit cannot be younger than the Late Proterozoic-Cambrian, because this ancient oceanic crust is intruded by the 750–540 Ma gabbro and diorite bodies of the Gray Granite Basement Complex (Table 8).

In light of these assumptions, we have examined mixing models (Langmuir et al., 1978; DePaolo, 1981) for element pairs of different incompatibility and their ratios, and the Nd isotopic ratios of the metabasic series (Fig. 6). The results argue against the mixing of two different melts as well as two distinct mantle sources. We interpret this to mean that the obtained isotopic variations point to the derivation of the metabasic series in the Tectonic Mélange Zone from a common mantle source that was depleted in Nd isotopic compositions ($\varepsilon Nd_{804}=7.37\pm0.55$). The assumption that all measured samples are cogenetic along with an evidence of $MSWD>1+2(2/f)^{1/2}$ statistical test ($1.73<2.62$; Wendt and Carl, 1991) indicates that the isotopic variation in $^{147}Sm/^{144}Nd$–$^{143}Nd/^{144}Nd$ for the metabasic series in the TCM carries an age significance. However, the strong fractionation of REE may reflect the age of the partial melting event of the source and not the emplacement age (Donnely et al., 2004). In this relation, we interpret the obtained isochron result to indicate a maximum age limit of the analyzed lithospheric fragments. The

Table 4
Major and trace element abundances of the gabbro–diorite–quartz diorite series of the Gray Granite Basement Complex

Sample no	68-84	UK-53	UK-115	T-289	3439	A-832	LG-3	GZ-1
SiO_2	49.30	55.85	59.76	63.62	64.58	66.07	59.93	65.83
TiO_2	0.79	1.18	1.12	0.57	0.85	0.46	0.88	0.98
Al_2O_3	16.70	17.52	18.01	16.16	16.30	14.59	17.36	15.70
FeO	8.00	6.99	6.61	5.69	5.68	5.34	7.89	6.08
MnO	0.14	0.11	0.08	0.10	0.08	0.16	0.20	0.08
MgO	5.80	4.67	3.20	0.98	3.00	2.54	3.81	1.79
CaO	6.80	3.49	4.71	3.25	3.69	3.06	2.96	4.82
Na_2O	1.90	3.24	2.97	3.81	2.71	2.46	2.67	2.00
K_2O	1.60	2.52	1.95	3.25	2.53	2.32	0.96	1.48
P_2O_5	0.12	0.33	0.33	0.17	0.27	0.14	0.26	0.30
LOI	7.85	4.35	1.65	1.48	0.65	3.01	3.09	0.76
Total	99.00	100.25	100.39	99.07	100.34	100.15	99.67	99.51
Rb	60.0	112.0	96.0	69.0	108.0	30.0	39.5	90.8
Ba	–	–	473	2028	538	–	605	565
Sr	270	–	371	307	252	–	520	535
Zr	60	–	303	289	294	–	205	435
Y	13.0	–	24.0	34.0	18.0	–	16.1	14.9
Nb	–	–	13	11	12	–	–	–
Th	1.4	5.8	5.6	12.8	1	7.3	1.7	3.56
Ta	–	0.7	–	0.5	0.6	0.4	0.56	0.94
Hf	2.2	6.9	3.6	–	5.6	–	4.19	19
La	10.30	31.00	37.00	95.00	14.00	14.20	13.00	14.80
Ce	19.30	50.00	65.00	150.00	24.00	22.00	26.50	31.70
Pr	2.30	5.30	7.00	12.00	2.50	2.40	3.02	3.95
Nd	8.30	20.00	25.00	38.00	8.50	8.00	11.90	17.20
Sm	1.87	4.80	6.00	8.10	2.00	2.20	3.08	4.89
Eu	0.83	1.30	11.00	1.30	0.85	0.24	1.13	1.70
Gd	2.60	5.50	5.50	4.80	2.70	2.50	4.23	5.80
Tb	0.42	0.80	0.83	0.75	0.48	0.38	0.63	0.81
Dy	2.60	4.50	5.10	4.70	2.70	2.40	3.76	4.50
Ho	0.57	0.95	1.15	1.10	0.65	0.55	0.81	0.91
Er	1.60	2.80	3.00	3.10	1.80	1.50	2.20	2.37
Tm	0.25	0.37	0.45	0.48	0.28	0.25	0.34	0.33
Yb	1.40	1.80	2.50	2.70	1.70	1.30	1.75	1.62
Lu	0.22	0.32	0.41	0.49	0.27	0.21	0.30	0.25

upper age limit of these fragments is constrained by the Neoproterozoic–Cambrian age of the Gray Granite Basement Complex. The Neoproterozoic–Cambrian (~750–500 Ma) age of the diorite intrusions in the Gray Granite Basement Complex has been supported by the U–Pb zircon dates from the granodiorite and quartz diorite-plagiogranite migmatite rocks in the Dzirula salient (Bartnitsky et al., 1989). This age bracket has been confirmed by the whole-rock Rb–Sr isochrons (686±54 Ma and 538±53 Ma) for the gneissic and massive quartz diorites, respectively (Okrostsvaridze et al., 2002), and by our Sm–Nd mineral isochron age of 607±78 Ma (Table 6; Fig. 5b) for the subvolcanic amphibole gabbro (Sample D-4-87) body in the same salient. The upper age limit of deposition of the metasedimentary subunit in the Oldest Basement Unit is also inferred as the Neoproterozoic because of numerous xenoliths of these metasedimentary rocks in various intrusions of the Neoproterozoic–Cambrian Gray Granite Basement Complex.

A sample from a quartz diorite intrusion in the felsic series (Sample: 3439, from Khunevi in the Dzirula Salient; Table 7, Fig. 5c) has revealed a young age of 198±30 Ma, indicating that some diorite bodies in the Gray Granite Basement Complex may correspond to the Upper Triassic–Lower Jurassic magmatic events, represented by up to 200–600 m-thick high-silica dacites and rhyolites that occur in the sedimentary cover of the Transcaucasian Massif (Lordkipanidze et al., 1989; Svanidze et al., 2000).

5. Discussion

5.1. Island arc evolution of TCM

The Gray Granite Basement Complex of TCM displays evidence for a prolonged (~200 m.y.) and complex evolutionary history during the Neoproterozoic–Early Cambrian (~750–540 Ma). Repeated emplacement of melts of basic to felsic

Table 5
WR Sm–Nd isotopic data for metabasalts for the Tectonic Melange Zone Transcaucasian massif*

Sample no	Sm	Nd	$^{147}Sm/^{144}Nd$	$^{143}Nd/^{144}Nd$	$\varepsilon Nd(T)$
47-84	4.03	11.5	0.2119±.0006	0.51234±.00005	8.09
49-84	2.07	5.56	0.2256±.0007	0.51236±.00004	7.07
50-84	1.82	4.82	0.2281±.0007	0.51237±.00011	7.01
57-84	3.33	9.86	0.2045±.0006	0.51223±.00004	6.70
71-84	4.94	22.1	0.1351±.0004	0.51189±.00005	7.17

*Measured Nd isotope ratios were normalized to 150Nd/142Nd=0.209627 (Wasserburg et al., 1981; Karpenko et al., 1984).

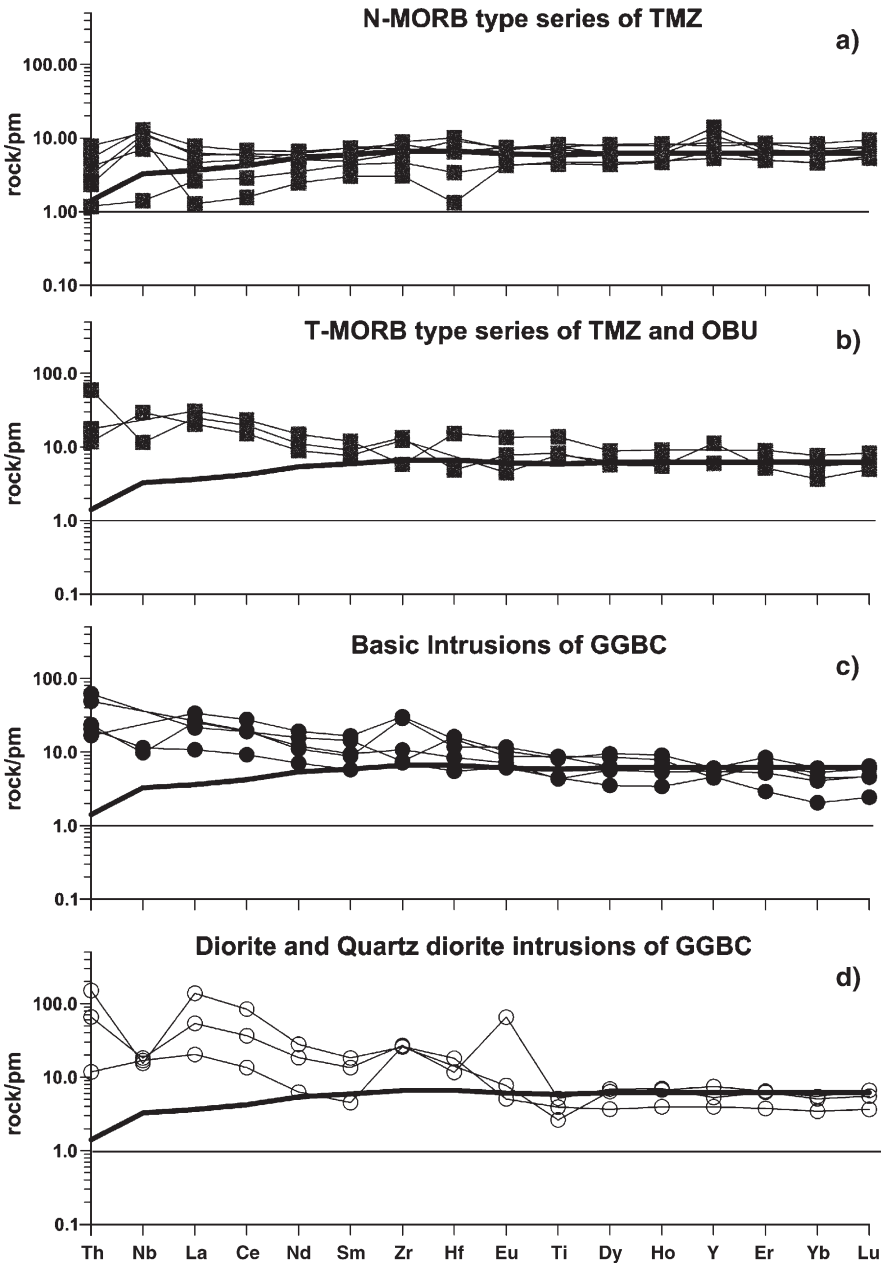

Fig. 4. Primordial mantle-normalized incompatible trace element abundance patterns of the Neoproterozoic–Early Cambrian basement units in the Transcaucasian Massif. a. N-MORB- and b. T-MORB-type series (amphibolites) of the Tectonic Mélange Zone (TMZ) and the Oldest Basement Unit (OBU), c. Subvolcanic basic intrusions (gabbros, diorites), d. Coarse-grained diorite-quartz diorite series (gabbros, diorites, quartz diorites, granodiorites, low-K granites), both from Gray Granite Basement Complex . Thick curve denotes an average N-MORB. Primordial mantle and N-MORB compositions are from (Sun and McDonough, 1989).

compositions, their fractionation patterns, and the assimilation of the Oldest Basement Unit rocks into these melts resulted in the formation of various diorite and quartz diorite intrusions, which were subsequently metamorphosed to diorite gneisses. The spatially and temporally associated diorite-quartz diorite intrusions in the Gray Granite Complex display common, continuous, and overlapping trends transitional from island arc

Table 6
Sm–Nd isotopic data of subvolcanic amphibole gabbro (D-4-87) of Gray Granite Basement Complex, Dzirula salient

Mineral	Sm	Nd	$^{147}Sm/^{144}Nd$	$^{143}Nd/^{144}Nd$
Plagioclase	0.55	8.1	0.1099±.0003	0.51156±.00002
Apatite	4.2	53.7	0.1267±.0004	0.51163±.00002
Amphibole 1	2.88	30.0	0.1553±.0005	0.51174±.00002
Amphibole 2	2.73	28.6	0.1545±.0005	0.51174±.00002

Table 7
Sm–Nd isotopic data of quartz diorite (3439) of Gray Granite Basement Complex, Dzirula salient

Mineral	Sm	Nd	$^{147}Sm/^{144}Nd$	$^{143}Nd/^{144}Nd$
Plagioclase	0.64	4.6	0.2255±.0007	0.51155±.00002
Biotite	0.16	6.2	0.1622±.0005	0.51149±.00002
Apatite	18	340	0.086±.0003	0.51137±.00002

tholeiitic to calc-alkaline series with predominantly basic to intermediate compositions (~80–85%). These intrusive rocks show LILE enrichment patterns, well-defined negative Ta, Nb, and Ti anomalies, narrow limits and identical values of characteristic trace element ratios (La/Ta=32±12; Hf/Ta=8.25±2.07; Th/Yb=2.45±1.5; Th/Hf=0.65±0.35) for the same fractionation interval. The low Sr/Y (15±4) and [$(La/Yb)_n$=6.55±2.2] and high Y and Yb contents [$(Yb)_n$=4.05±1.1; $(Y)_n$=4.29±1.80] (Fig. 7b) along with varying Eu anomalies indicate plagioclase control and preclude the involvement of high-pressure phases such as garnet and amphibole in the fractionation process during the evolution of the Gray Granite Complex (Drummond and Defant, 1990). The compositional overlap (Figs. 4 and 7) between the coarse-grained gabbro, diorite, and quartz diorite intrusions in the Gray Granite Complex indicates a genetic relationship, suggesting that they probably formed as part of the same island arc complex.

The available Nd and Sr isotope data (Okrostsvaridze et al., 2002; Zakariadze and Karpenko, unpublished data) from the Gray Granite Basement Complex are shown on a εNd versus εSr diagram (Fig. 7d). Almost all the data plot in the enriched field (high εSr, low εNd), indicating that the magmas of these series were generated at the expense of relatively LREE-enriched (low Sm/Nd and high Rb/Sr) sources, typical of continental crust. We can define two groups of isotopic ratios on this diagram. For the *first group*, which includes gabbro and diorite rocks, there is a close correlation of εNd and εSr values nearly along the mantle array. The variations of typical ratios for this group include εNd from +1.9 to −5.63, Sm/Nd=0.194±0.03, and $^{87}Sr/^{86}Sr_{int}$ 0.704247–0.705417. The *second group*, which consists of massive quartz diorites, has similar Nd values but much higher Sr isotopic ratios compared to the first group, and shows isotopic ratios of εNd(T) from −2.02 to −5.62; Sm/Nd=0.194±0.03; and $^{87}Sr/^{86}Sr_{int}$ 0.708618–0.708773. The model T_{DM}(Nd) ages for the whole Gray Granite Basement Complex vary in relatively narrow limits (T_{DM}=1387±176 Ma), and the difference between the model and emplacement ages is rather high (775±220 Ma). All these data collectively point to a potential involvement of continental crust during the igneous accretion of the Gray Granite Basement Complex. However, the geochemical features of the Gray Granite Basement Complex are also characteristic of ensimatic arc sequences developed in intra-oceanic settings. The MORB-type mafic–ultramafic rocks in the Old Basement Unit and in the Tectonic Mélange Zone are interpreted to have formed the oceanic basement of this inferred arc complex, represented by the Gray Granite Basement Complex. The closest modern analogue for this inferred Neoproterozoic arc system is the Lesser Antilles island arc, whose igneous evolution involved continental crustal contribution to subduction-metasomatized, mantle-derived melts (Davidson, 1986; White and Dupre, 1986).

5.2. Pan-African origin of TCM and implications for the evolution of ANS Crust

The geological, geochronological, and geochemical characteristics of the Oldest and Gray Granite Basement Units of the TCM are analogous to those of the Neoproterozoic island arc complexes of the Arabian–Nubian Shield (ANS) that formed during the Pan-African period in the aftermath of the break-up of the supercontinent Rodinia. The Neoproterozoic volcanic arcs and composite arc terranes in the ANS are separated by several NE-trending ophiolitic suture zones that range in age from 870 Ma to 627 Ma (Abdelsalam and Stern, 1996; Dilek and Ahmed, 2003; Johnson et al., 2004, and references therein). These volcanic arc terranes were incorporated into the ANS through a series of collisional events prior to the terminal closure of the Mozambique Ocean that resulted in the collision of East and West Gondwana during the Neoproterozoic (Dalziel, 1997). The volcanic arc terranes in the ANS appear to become progressively younger from south (e.g., Asir and Haya terranes, >900–800 Ma) to north (e.g., Midyan and Dokhan terranes, ~700–600 Ma). Most of these arc terranes have poly-phase magmatic accretion histories and show tholeiitic to calc-alkaline evolutionary trends through time (Camp, 1984; Vail, 1985; Stoeser and Camp, 1985). Isotopic studies of disrupted ophiolitic units structurally underlying the volcanic arc complexes and in the suture zones suggest that the Neoproterozoic arc assemblages in the ANS were commonly built on a deformed oceanic basement (Pallister et al., 1988; Kröner et al., 1992). However, based on limited current isotopic data, we infer that the pre-Pan-African continental crust was also involved in the formation of juvenile arc material in the ANS. The typical intervals of isotopic ratios of εNd(T) and $^{87}Sr/^{86}Sr_{int}$ (8.71 to −15.8, and 0.70194 to 0.72304, respectively) from the TCM are

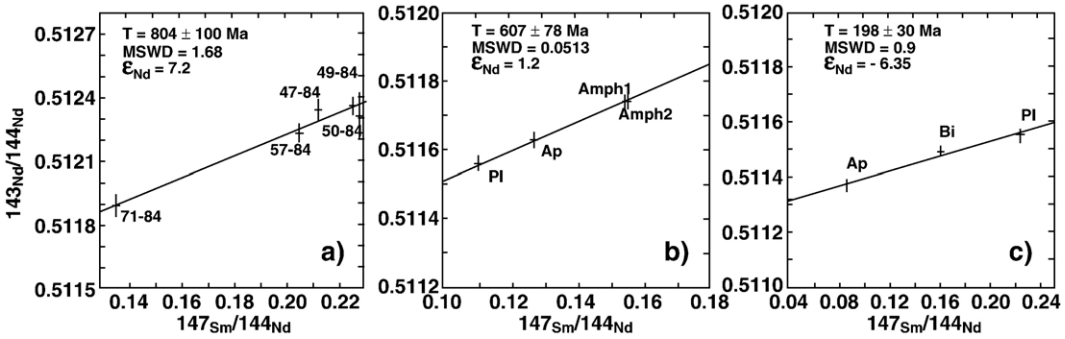

Fig. 5. $^{147}Sm/^{144}Nd$ –$^{143}Nd/^{144}Nd$ plot for the crystalline basement units in the Transcaucasian Massif. (a) Whole-rock isochron for metabasalts from the Tectonic Mélange Zone (TMZ), (b) Mineral isochron for a subvolcanic amphibole-gabbro (Sample # 4-87), Dzirula salient, (c) Mineral isochron for a quartz-diorite (Sample # 3439), Dzirula salient (amphibole-gabbro and quartz-diorite samples are both from the Gray Granite Basement Complex).

similar to those reported from the ANS arc complexes (Harris et al., 1984; Pallister et al., 1988; Sultan et al., 1990; Lenoir et al., 1994; Stern, 1994; Harms et al., 1994) and also indicate the involvement of continental crust in the island arc evolution of the ANS. The involvement of pre-Pan African crust in the evolution of the ANS has been also suggested by some other researchers, as well (Dixon, 1981; Stacey and Hedge, 1984; Sultan et al., 1992); more systematic geochronological studies are needed, however, to better document the extent of this involvement. The approximate crust–mantle budget for the Neoproterozoic arc complexes in the TCM and the ANS, based on simple two component mixing models (DePaolo, 1981; DePaolo et al., 1991; Asmeron et al., 1991), shows possible mantle additions of up to 65% to 72%. The most significant mantle input is shown by the gabbro-diorite-quartz diorite rocks of the Gray Granite Basement Complex in TCM with the highest εNd and the lowest $^{87}Sr/^{86}Sr$ ratios (−5.63 to +1.9, and 0.70455 to 0.70542, respectively).

The field, geochronological, and geochemical data from the Neoproterozoic TCM and ANS volcanic arc complexes thus show that island arc construction in the Arabian–Nubian Shield involved the contribution of continental crust. Therefore, the ANS was not made entirely of juvenile arc material as some of the previous studies have suggested (Stern and Hedge, 1985; Kröner et al., 1994). Recent findings from Neoproterozoic island arc complexes (~770–720 Ma) in the Eastern Desert of Egypt (Farahat et al., 2004) also support this interpretation and document the involvement of the pre–Pan-African continental crust in the evolution of depleted mantle-derived magmas during the evolution of the ANS arc–backarc crust.

5.3. Tectonic evolution of the TCM within the Gondwana and Eurasia realms

The geological history of the TCM is depicted in a simple columnar section in Fig. 8. We identify four major evolutionary phases in the Neoproterozoic–Jurassic history of the TCM. The ancient foundation of the TCM, represented by the Neoproterozoic–Early Cambrian island arc complex, was generated in a ~200 m.y. time period when the TCM was still part of Western Gondwana. The magmatic and metamorphic events that affected the TCM during <800 Ma and 600 Ma were part of the tectonic evolution Western Gondwana as the supercontinent Rodinia was being dismantled. Igneous and metamorphic events of this age bracket have not been documented from the East European Platform and the Schytian and Moesian blocks in southern Eurasia (Adamia et al., 1981; Adamia, 1984; Khain and Bozhko, 1988; Haydoutov et al., 1997; Haydoutov and Yanev, 1997; Chen et al., 2002; Murphy et al., 2004).

The pre-Carboniferous and post-Neoproterozoic (after ~600 Ma) geological history of the TCM is partially recorded in the metasedimentary rock units of the Tectonic Mélange Zone. This time window during the Paleozoic corresponds to the evolution of the Paleo-Tethys after the fragmentation of the northern edge of Western Gondwana (Stern, 1994), the passive margin evolution of the TCM (Fig. 8), and the deposition of the Lower-Middle Paleozoic strata locally exposed as tectonic slices within the Tectonic Mélange Zone (Adamia et al., 1987). The TCM escaped the latest episodes of the Pan-African metamorphic and deformation events (~550 Ma) because it was already rifted away from ANS (Gondwana) by that time.

Table 8
Geochronology of crystalline basement rocks in the main tectonic units of the Transcaucasian Massif

Tectonic Unit	Lithology	Age (Ma)	Dating technique	References
Oldest Basement Unit	Amphibolite (metabasic rocks)	804±100	Sm/Nd mineral isochron	This study
Gray Granite Basement Complex	Quartz diorite, plagiogranite, gneissic, granodiorite (Dzirula salient)	750–490	U/Pb zircon	Bartnitsky et al., 1989
	Gneissic quartz diorite (Dzirula salient)	686±54	Rb/Sr whole-rock	Okrostsvaridze et al., 2002
	Massive quartz diorite	538±53	Rb/Sr whole-rock	Okrostsvaridze et al., 2002
	Amphibole gabbro	607±78	Sm/Nd mineral isochron	This study
Tectonic Mélange Zone	Amphibolite and metabasic rocks	804±100	Sm/Nd mineral isochron	This study
	Phyllite (sedimentary cover of metaophiolite)	Cambrian–Upper Devonian	Stratigraphy	Abesadze et al., 1980

The emplacement of the Middle-Late Carboniferous microcline granite intrusions (Microcline Granite Basement Complex) into the ancient foundation of the TCM occurred nearly 300 million years later and constituted the main phase of continental crustal growth of the TCM, making up more than 50% of its crystalline basement. The 330–280 Ma microcline granite rocks in the TCM geochemically represent VAG-type (volcanic arc granite) intrusions (Zakariadze, unpublished data) characteristic of active continental margins and are widespread throughout the Caucasus (Transcaucasus, Great Caucasus, and Precaucasus). The emplacement of these Late Paleozoic Microcline Granite series was a significant magmatic episode during the evolution of the Eurasian active continental margin above a north-dipping (in present coordinate system) Paleo-Tethyan subduction zone. They occur in the Balkan Sector of the Variscan orogen in central Bulgaria (Carrigan et al., 2005), the Pelagonian Zone of the Internal Hellenides in Greece (Anders et al., 2006), and the Strandja massif in Thrace of NW Turkey (Okay et al., 2001; Natal'in et al., 2005). Thus, the TCM was already part of the southern Eurasian continental margin by the Early Carboniferous (~350 Ma).

The suturing of the TCM into the Eurasian continental margin was completed by 330 Ma and was followed by the emplacement of the Microcline Granite series (Shavishvili, 1983; Adamia, 1984; Khain, 1984; Somin, 1991). The TCM was situated in the upper plate of the Paleo-Tethyan subduction zone throughout the Late Paleozoic and earliest Mesozoic. Starting in the Upper Triassic, the continental rifting and passive

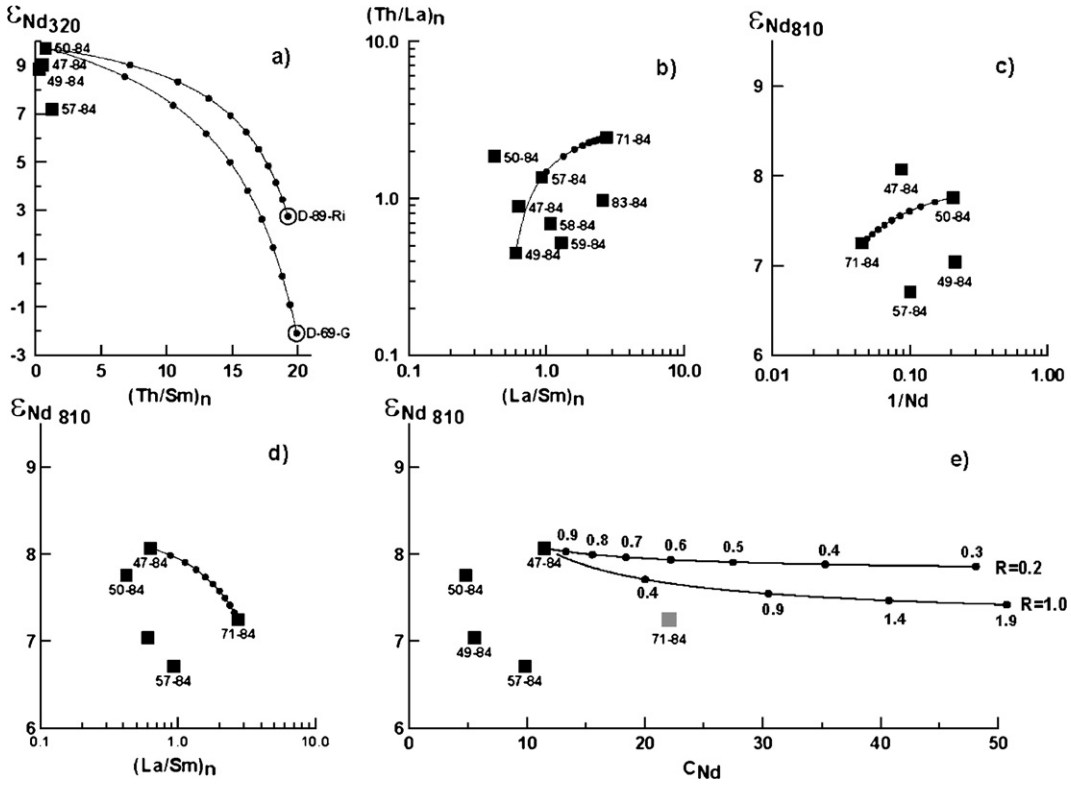

Fig. 6. εNd and trace-element ratios, mixing relation plots for the MORB-type metabasaltic rocks from the Tectonic Mélange Zone (CHUZ) in the Dzirula salient. (a) relations of MORB-type basalts with typical compositions of the Middle-Late Carboniferous granites (Samples D-69-G: microcline granite and D-89-Ri: rhyolite), (b–d) relations of variously LREE-enriched metabasalts, (e) AFC fractionation curves (DePaolo, 1981) for the basalt (Sample #47-84 [$(La/Sm)_n=0.63$]) to which batches of the enriched basaltic melt (Sample #71-84 [$(La/Sm)_n=2.47$]) were added. The model was calculated for the liquidus association $Ol_{8.7}+Pl_{25.3}+Cpx_{6.2}$ of the basalt (Sample # 47-84; MgO=7.5 wt.%) and K_d values of Bédard, 1994). $R=Ma_a/M_c$ is the ratio of rates of assimilation processes (the involvement of the composition of Sample # 71-84) and crystallization of the basalt (Sample # 47-84). The values at the curve $R=0.2$ — variation of the mass of crystallized melt. The values at the curve $R=1$ — the ratio Ma_a/M_m of the rate of involvement of enriched melt to total mass of crystallizing melt.

margin evolution associated with the opening of Neo-Tethys dominated the tectonic evolution of the Eastern Pontides and the Caucasus (Okay and Sahintürk, 1997; Yilmaz et al., 1997; Zakariadze et al., 2005). The rift strata in the region include shallow-water sedimentary rocks intercalated with volcanic, volcaniclastic, and pyroclastic rocks having tholeiitic basaltic, andesitic, and rhyolitic compositions (Fig. 8).

5.4. Other Peri-Gondwanan Terranes with Pan-African Origin in Eastern Europe

Recent studies in the eastern Mediterranean region have shown the existence of peri-Gondwanan terranes with Pan-African origin in places within the broader Alpine orogenic belt where significant crustal uplift and/or post-collisional crustal exhumation exposed these Late Precambrian rocks. The Danubian pre-Alpine basement in the South Carpathians (Romania) contains a ~777±3 Ma island arc complex (Dragsan Group) whose rocks display tholeiitic to more differentiated, low-K calc-alkaline trends (Liégeois et al., 1996), analogous to the early Pan-African juvenile arc terranes. Farther south in the Protomoesian microcontinent in Bulgaria, a Neoproterozoic–Cambrian ophiolite-island arc assemblage is unconformably overlain by a Middle Ordovician sedimentary sequence (Haydoutov and Yanev, 1997). The arc plutons are intrusive into the ophiolitic units indicating that the Neoproterozoic arc-ophiolite assemblage represents an ensimatic arc terrane reminiscent of many of the Late Precambrian arc terranes in the Arabian–Nubian Shield (e.g., Hijaz and Jiddah terranes; Dilek and Ahmed, 2003; Johnson et al., 2004). The ophiolitic suture zone separating the Balkan and Thracian terranes in southern Bulgaria includes a tectonic mélange zone (Diabase Phyllitoid Complex) that is composed of MORB-type meta-ophiolites tectonically imbricated with 660–545 Ma island arc units (Struma Diorite Formation; Haydoutov et al., 1993, 1994; Zagorchev, 2000; Savov et al., 2001). This mélange zone is similar in terms of its lithological units, internal structure, and age relations to the Tectonic Mélange zone in the TCM.

The Pelagonia ribbon-continent in Greece contains orthogneisses with SHRIMP ages ranging from 699±7 Ma to 713±18 Ma, and the granitic protoliths of these Neoproterozoic basement rocks show trace-element geochemistry characteristic of volcanic arcs (Anders et al., 2006). The occurrence of inherited zircons with Mesoproterozoic ages (Anders et al., 2006) in these metamorphosed arc rocks suggests formation of the Neoproterozoic arc complex close to a continental margin, likely Gondwana. The Strandja massif in SE Bulgaria and NW Turkey also includes granitic orthogneisses with calc-alkaline chemical trends and ages of 650 Ma (Natal'in et al., 2005).

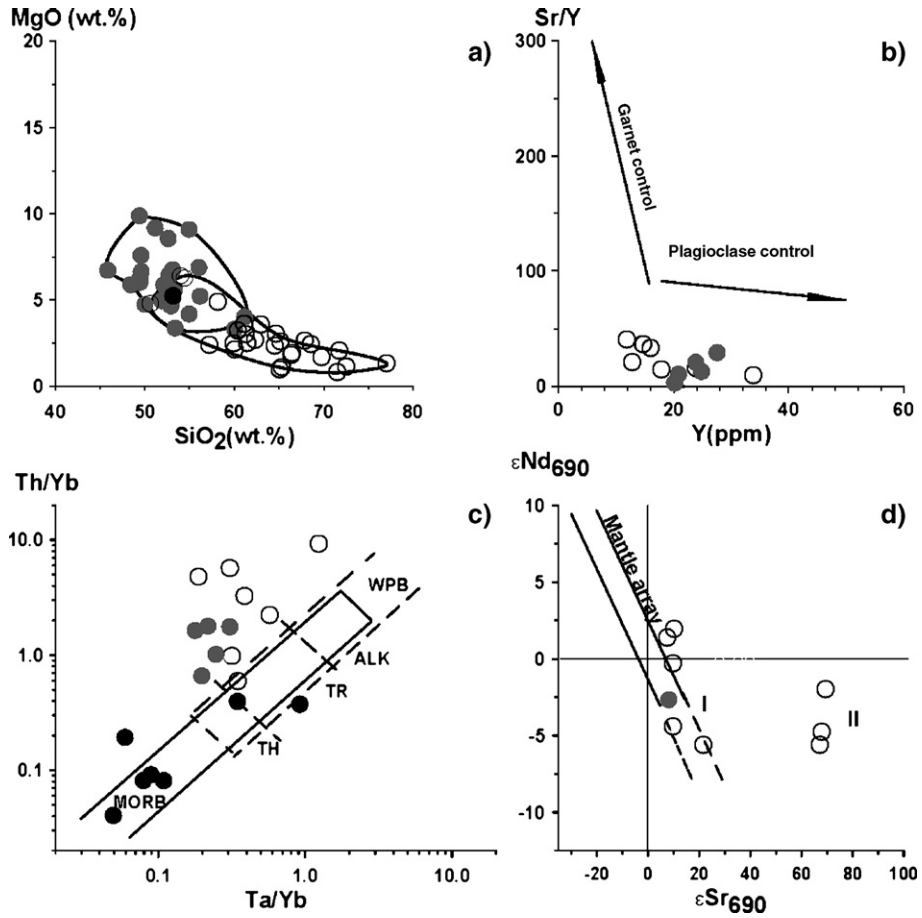

Fig. 7. Representative plots of the compositions of the sub-volcanic basic intrusions and coarse-grained diorite and quartz-diorite series in the Gray Granite Basement Complex. Th/Yb–Ta/Yb diagram is from Alabaster et al. (1982). Filled circles = basic intrusions; open circles = diorites and quartz diorites.

Both the Pelagonia continent and the Strandja massif are interpreted to have been rifted away from Gondwana in the Early Cambrian and to have been accreted into the southern margin of Eurasia where they became part of the basement of a Permo-Carboniferous magmatic arc above a Paleo-Tethyan subduction zone (Sengör and Natal'in, 1996; Anders et al., 2006).

The occurrence of Neoproterozoic peri-Gondwanan fragments in the crystalline basement of the Alpine orogenic belt along a nearly E–W-trending zone stretching from the Alps to the Caucasus may have resulted from their near coeval rifting from the northern edge of Gondwana in the Early Paleozoic. Recent studies and paleogeographic reconstructions suggest that this rifting event may have been associated with a back-arc extension above a south-dipping (in present coordinate system) subduction zone (Neubauer, 2002; Nance et al., 2002; Gürsu and Göncüoglu, 2005). The magmatic arc of this subduction zone is probably represented by the ~590–570 Ma Istanbul–Zonguldak Zone in northern Turkey (Yigitbas et al., 2002). The Early Cambrian mafic volcanic rocks and dikes associated with the Lower Paleozoic metapelites in the western Taurides in southern Turkey may represent the early products of this back-arc extension (Gürsu and Göncüoglu, 2005). Continued rifting and seafloor spreading within this back-arc environment led to the development of the Paleo-Tethyan Ocean (Neubauer, 2002; Nance et al., 2002).

6. Conclusions

The crystalline basement of the Transcaucasian Massif consists of two major units. The MORB-type metabasic rocks (804±100 Ma; εNd_{int}=7.37±0.52) occurring in the Oldest Basement Unit and in the Tectonic Mélange Zone represent fragments of a Neoproterozoic oceanic lithosphere. The mafic to intermediate plutons (~750–540 Ma) intruding this ancient oceanic lithosphere constitute the Gray Granite Basement Complex and represent an island arc complex developed on an oceanic substratum. The Oldest Basement Unit and the Gray Granite Basement Complex collectively form a Neoproterozoic–Early Cambrian ensimatic arc terrane, which is likely to have been derived from the Arabian–Nubian Shield of Western Gondwana based on the similarities of the internal structure, age relations, and geochemical features of its arc-ophiolite units with those in the ANS. Magmatic and metamorphic events that produced the Neoproterozoic–Early Cambrian rocks of the TCM are missing from the geological record of southern Eurasia.

The Nd and Sr isotopic ratios of the island arc plutons in the TCM (Gray Granite Basement Complex) and the significant time

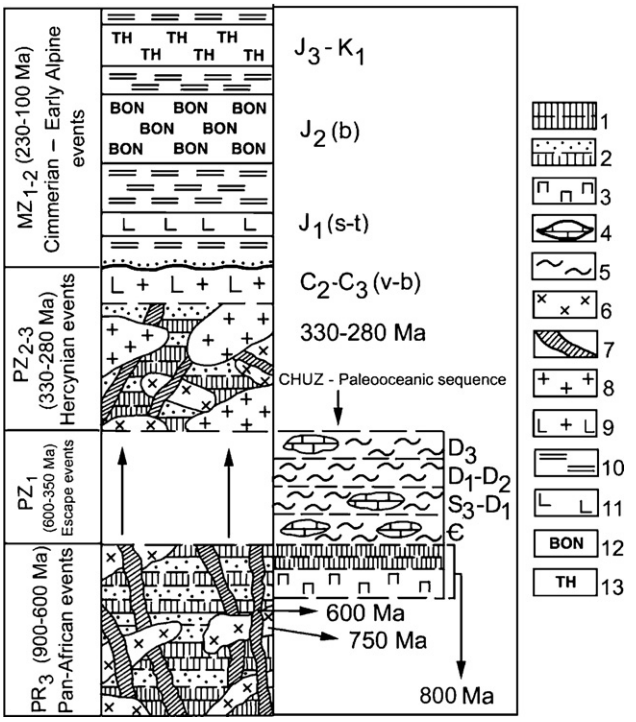

Fig. 8. Simplified columnar section of the Transcaucasian Massif, depicting its geological history spanning the Late Proterozoic– Early Mesozoic time window. Key to numbering: 1. Metabasic series of the Oldest Metabasic-Plagiogneiss-Migmatite-Basement Unit, 2. Metasedimentary series of the Oldest Metabasic-Plagiogneiss-Migmatite-Basement Unit, 3. Serpentinized peridotites, 4. Marble lenses, 5. Phyllites in the Tectonic Mélange Zone (CHUZ). 6. Gabbroic, dioritic and quartz-dioritic intrusions, 7. Subvolcanic basic intrusions, 8. Microcline granite intrusive bodies, 9. Subaerial rhyolites and rhyodacites, 10. Jurassic shallow-water sedimentary rocks, 11. Triassic–Lower Jurassic (T_3–J_1) rhyolites, 12. Bajocian boninitic series, 13. Bathonian–Hauterivian tholeiitic andesites.

difference between their model and emplacement ages indicate the involvement of a pre-existing Mesoproterozoic continental crust in the igneous evolution of this ensimatic arc terrane. The subduction zones that facilitated the igneous accretion of the island arc terranes in the ANS may therefore have been in a close proximity to a continental mass (Western Gondwana), reminiscent of the evolution of the Jurassic ensimatic arc terranes in the western U.S. Cordillera (Dilek et al., 1991) and of the Lesser Antilles arc in the Caribbean region (Davidson, 1986; White and Dupre, 1986). This finding indicates that the Neoproterozoic crust of the ANS was not made entirely of juvenile arc material, as previous models have suggested.

The TCM, along with a series of other continental fragments that are now exposed in the Late Precambrian–Cambrian crystalline basement of the Alpine orogenic belt, was separated from Western Gondwana during the Early Paleozoic as a result of back-arc rifting above a south-dipping subduction zone. Continued rifting and seafloor spreading produced the Paleo-Tethys in the wake of northward migrating peri-Gondwanan terranes. The accretion of the TCM and other peri-Gondwanan terranes into the southern margin of Eurasia was completed by ~350 Ma. Widespread emplacement of microcline granite plutons along the active continental margin of southern Eurasia during 330–280 Ma occurred above a north-dipping Paleo-Tethyan subduction zone and marked a period of significant continental growth in the geological history of Eurasia.

The TCM and other peri-Gondwanan terranes currently exposed in the core of the Alpine orogenic belt provide an excellent opportunity to investigate the mode and nature of igneous, metamorphic, and tectonic processes that played a major role in the rapid crustal accretion of Gondwana in the Neoproterozoic and to better document the rift-drift-subduction history of Paleo-Tethys. Future systematic geochemical, isotopic, and geochronological studies of these peri-Gondwanan crystalline basement rocks should also contribute to our better understanding of the evolution of continental crust.

Acknowledgements

We are grateful to E.V. Bibikova, V.G. Kazmin, and Y.A. Kostitsyn for fruitful the discussions on the geology and geochemistry of the Transcaucasian Massif and on the results of our study, and to T. Kusky, and A. Polat, and R. Stern on the Precambrian tectonics in general. We also thank R.J. Stern for providing a thorough review of an earlier version of this paper. This research was supported by a RFBR Grant 05-05-64 125 to G. Zakariadze and by RFBR grant 04-05-64754 to B.A. Bazylev and a NATO grant (EST-EV.978184) and a Miami University Havighurst Centre Research Fund Grant to Y. Dilek. Thorough and critical journal reviews by Akira Ishiwatari and Mohamed Sultan improved the paper substantially. We wish to express our sincere thanks to Professor M. Santosh for inviting us to contribute this paper to the Special Issue of Gondwana Research on *Island Arcs: Past and Present*.

References

Abdelsalam, M.G., Stern, R.J., 1996. Sutures and shear zones in the Arabian-Nubian Shield. Journal of African Earth Sciences 23, 289–310.

Abesadze, M.B., Tsimakuridze, G.K., Planderova, E., 1980. New data on age of metamorphosed schists of Dzirula massif (Georgia). Geologicke Prace, Spravy 74, 137–144.

Abesadze, M.B., Adamia, Sh.A., Gabunia, G.L., et al., 1989. Pudding metaconglomerates of the Chorchana–Utslevi zone of Dzirula massif, their age and geological significance. Bulletin of the Academy of Sciences of the Georgian SSR 135, 129–132.

Adamia, Sh.A., 1984. Prealpine basement of the Caucasus — composition, structure, and formation. In: Otkhmezuri, Z.V. (Ed.), Tectonika i metallogenia Kavkaza, vol. 86. Metsniereba, Tbilisi, pp. 3–104.

Adamia, Sh.A., Shavishvili, I.D., 1979. Model of tectonic evolution of the Earth crust of the Caucasus and adjacent territory. Geotectonica 1, 77–84.

Adamia, Sh.A., Chkhotua, T., Kekelia, M., Lordkipanidze, M., et al., 1981. Tectonics of the Caucasus and adjoining regions: implications for the evolution of the Tethys ocean. Journal of Structural Geology 3, 437–447.

Adamia, Sh.A., Belov, A.A., Kekelia, M.A., Shavishvili, I.D., 1987. Paleozoic tectonic development of the Caucasus and Turkey (Geotraverse C). In: Flugel, H.W., Sassi, F.P., Grecula, P. (Eds.), Pre-Variscan and Variscan Events in the Alpine–Mediterranean Mountain BeltsMineralia Slovaca – Monography, Alfa Bratislava, pp. 23–50.

Adamia, Sh., Lordkipanidze M., Kvantaliani, I., Kutelia, Z., 1990. Geology of the Caucasus: a Guide of field meeting of the Working group 5.1. Paleogeography and tectonics of the Paleozoic fold areas and their platform frame. Geotraverse 10 (Caucasus), Tbilisi, September 1–6, 1990. Al. Djanelidze Geological Institute of the Academy of Sciences of GSSR. p. 39.

Alabaster, T., Pearce, J.A., Malpas, J., 1982. The volcanic stratigraphy and petrogenesis of the Oman ophiolite complex. Contributions to Mineralogy and Petrology 81, 168–183.

Anders, B., Reischman, T., Kostopulos, D., Poller, U., 2006. The oldest rocks of Greece: first evidence for a Precambrian terrane within the Pelagonian Zone. Geological Magazine 143, 41–58.

Asmeron, Y., Patchett, P.J., Damon, P.E., 1991. Crust–mantle interaction in continental arcs: inferences from the Mesozoic arc in the southwestern United States. Contributions to Mineralogy and Petrology 107, 124–134.

Bartnitsky, Ye.N., Dudauri, O.Z., Stepanyuk, L.M., 1989. Geochronology of Phanerozoic granitoids from folded areas of Eastern Europe. 5th Working Meeting, Isotopes in Nature, Leipzig, September. Proceedings, pp. 1–10.

Bédard, J.H., 1994. A procedure for calculation the equilibrium distribution of trace elements among the minerals of cumulate rocks, and the concentration of trace elements in the coexisting liquids. Chemical Geology 118, 143–153.

Camp, V.E., 1984. Island arcs and their role in the evolution of the Western Arabian Shield. Geological Society of America Bulletin 195, 913–921.

Carrigan, C.W., Mukasa, S.B., Haydoutov, I., Kolcheva, K., 2005. Age of Variscan magmatism from the Balkan sector of the orogen, central Bulgaria. Lithois 82, 125–147.

Chen, F., Siebel, W., Satir, M., Terzioglu, M.N., 2002. Geochronology of the Karadere basement (NW Turkey) and implications for the geological evolution of the Istanbul zone. International Journal of Earth Sciences (Geologische Rundschau) 91, 469–481.

Dalziel, I.D., 1997. Overview: Neoproterozoic–Paleozoic geography and tectonics: review, hypothesis, environmental speculation. Geological Society of America Bulletin 109, 16–42.

Davidson, J.P., 1986. Isotopic and trace element constraints on the petrogenesis of subduction-related lavas from Martinique, Lesser Antilles. Journal of Geophysical Research 91, 5943–5962.

DePaolo, D.J., 1981. Trace element and isotopic effects of combined wall rock assimilation and fractional crystallization. Earth and Planetary Science Letters 53, 189–202.

DePaolo, D.J., Linn, A.M., Schubert, G., 1991. The continental crustal age distribution: methods of determining mantle separation ages from Sm–Nd isotopic data and application to the southwestern United States. Journal of Geophysical Research 96, 2071–2088.

Dick, H.J.B., Bullen, T., 1984. Chromian spinel as a petrogenetic indicator in abyssal and alpine-type peridotites and spatially associated lavas. Contributions to Mineralogy and Petrology 86, 54–76.

Dilek, Y., Ahmed, Z., 2003. Proterozoic ophiolites of the Arabian Shield and their significance in Precambrian tectonics. In: Dilek, Y., Robinson, P.T. (Eds.), Ophiolites in Earth History. Geological Society of London Special Publications, vol. 218, pp. 685–700.

Dilek, Y., Thy, P., Moores, E.M., 1991. Episodic dike intrusions in the northwestern Sierra Nevada, California: implications for multistage evolution of a Jurassic arc terrane. Geology 19, 180–184.

Dixon, T., 1981. Age and chemical characteristics of some pre-Pan-African rocks in the Egyptian Shield. Precambrian Research 14, 119–133.

Donnely, K.E., Goldstein, S.L., Langmuir, Ch.H., Spiegelman, M., 2004. Origin of enriched ocean ridge basalts and implications for mantle dynamics. Earth and Planetary Science Letters 226, 347–366.

Drummond, M.S., Defant, M.J., 1990. A model for trondhjemite–tonalite–dacite genesis and crustal growth via slab melting: Archean and modern comparisons. Journal of Geophysical Research 95, 503–521.

Farahat, E.S., El Mahalawi, M.M., Hoinkes, G., Abdel Aal, A.Y., 2004. Continental back-arc basin origin of some ophiolites from the Eastern Desert of Egypt. Mineralogy and Petrology 82, 81–104.

Gamkrelidze, I.P., Shengelia, D.M., 1999. The new data about geological structure of the Dzirulla crystalline massif and the conditions of formation of magmatites. Proceedings of Geological Institute of Academy of Sciences Georgia, New Series 114, 46–71.

Gamkrelidze, I.P., Dumbadze, G.D., Kekeliya, M.A., et al., 1981. Ophiolites of the Dzirula massif and the problem of the Paleotethys on the Caucasus. Geotektonika 5, 23–33.

Gamkrelidze, I.P., Shengelia, D.M., Shvelidze, Iu.U., Vashakidze, G.T., 1999. The new data about geological structure of the Lokhi crystalline massif and Gorastskali metaophiolites. Proceedings of Geological Institute of Academy of Sciences Georgia, New Series 114, 82–108.

Gürsu, S., Göncüoglu, M.C., 2005. Early Cambrian back-arc volcanism in the western Taurides, Turkey: implications for rifting along the northern Gondwanan margin. Geological Magazine 142, 617–631.

Harms, U., Darbyshire, D.P.F., Denkler, T., Hengst, M., Schandelmeier, H., 1994. Evolution of the Neoproterozoic Delgo suture zone and crustal growth in Northern Sudan: geochemical and radiogenic isotope constraints. International Journal of Earth Sciences (Geologische Rundschau) 83, 591–603.

Harris, N.B.W., Hawkesworth, C.J., Ries, A.C., 1984. Crustal evolution in northeast and east Africa from model Nd ages. Nature 309, 773–776.

Haydoutov, I., Yanev, S., 1997. The Protomoesian microcontinent of the Balkan Peninsula — a peri-Gondwanaland piece. Tectonophysics 272, 303–313.

Haydoutov, I., Daieva, L., Kolcheva, K., 1993. Ophiolite blocks in the Diabase–Phyllitoid Complex from SW Bulgaria. Review of the Bulgarian Geological Society LIV 3, 60–70.

Haydoutov, I., Kolcheva, K., Daieva, L., 1994. The Struma Diorite Formation from Vlahina block, SW Bulgaria. Review of the Bulgarian Geological Society 55 (3), 9–35 (in Bulgarian with English summary).

Haydoutov, I., Gochev, P., Kozhoukharov, D., Yanev, S., 1997. Terranes in the Balkan Area. In: Papanikolaou (Co-r). IGCP Project No 276 Paleozoic geodynamic domains and their alpidic evolution in the Tethys. TERRANE MAPS AND TERRANE DESCRIPTIONS 479–494.

Johnson, P.R., Kattan, F.H., Al-Saleh, A.M., 2004. Neoproterozoic ophiolites in the Arabian Shield: field relations and structure. In: Kusky, T.M. (Ed.), Precambrian Ophiolites and Related Rocks. Developments in Precambrian Geology, vol. 13. Elsevier, pp. 129–162.

Karpenko, S.F., Sharas'kin, A. Ya., Balashov, Yu. A., et al., 1984. Isotopic and geochemical criteria for boninite origin. Geokhymiya 7, 958–970.

Khain, E.V., 1984. Ophiolites and Hercynian Nappe Structure of the Fore Range of the Northern Caucasus. Nauka, Moscow. 95 pp.

Khain, V.E., Bozhko, N.A., 1988. Historical Geotectonics. Precambrian. Nedra, Moscow. 380 pp.

Korikovsky, S.P., 1979. Metamorphic Facies of Metapelites. Nauka, Moscow, p. 255.

Kröner, A., Todt, W., Hussein, I.M., Mansour, M., Rashwan, A.A., 1992. Dating of late Proterozoic ophiolites in Egypt and Sudan using the single grain zircon evaporation technique. Precambrian Research 59, 15–32.

Kröner, A., Krüger, J., Rashwan, A.A., 1994. Age and tectonic setting of granitoid gneisses in the Eastern Desert of Egypt and SW Sinai. Geologische Rundschau 83, 502–513.

Langmuir, C.H., Vosche, R.D., Hanson, G.H., 1978. A general mixing equation with application to Icelandic basalts. Earth and Planetary Science Letters 37, 380–392.

Lenoir, J-L., Kuster, D., Liegeois, J.-P., Utke, A., Haider, A., Matheis, G., 1994. Origin and regional significance of late Precambrian and early Palaeozoic granitoids in the Pan-African belt of Somalia. International Journal of Earth Sciences (Geologische Rundschau) 83, 624–641.

Liégeois, J.P., Berza, T., Tatu, M., Duchesne, J.C., 1996. The Neoproterozoic Pan-African basement from the Alpine Lower Danubian nappe system (South Carpathians, Romania). Precambrian Research 80, 281–301.

Lordkipanidze, M.B., Meliksetian, B., Djarbashian, R., 1989. Mesozoic–Cenozoic magmatic evolution of the Pontian–Crimean–Caucasian region. In: Rakus, M., Dercourt, J., Nairn, A.E.M. (Eds.), Evolution of the Northern Margin of TethysThe Results of IGCP 198, Occasional Publications ESRI, New Series, vol. 4, pp. 103–131.

Murphy, J.B., Pisarevsky, S.A., Nance, R.D., Keppie, J.D., 2004. Neoproterozoic–Early Paleozoic evolution of peri-Gondwanan terranes: implications for Laurentia–Gondwana connections. International Journal of Earth Sciences (Geologische Rundschau) 93, 659–682.

Nance, R.D., Murphy, J.B., Keppie, J.D., 2002. A Cordilleran model for the evolution of Avalonia. Tectonophysics 352, 11–31.

Natal'in, B., Sunal, G., Toraman, E., 2005. The Strandja arc: anatomy of collision after long-lived arc parallel tectonic transport. In: Sklyarov, E.V. (Ed.), Structural and Tectonic Correlation Across the Central Asia Orogenic Collage: North-Eastern Segment. Guidebook and Abstract Volume of the Siberian Workshop IGCP-480. IEC SB RAS, Irkutsk, pp. 240–245.

Neubauer, F., 2002. Evolution of late Neoproterozoic to early Paleozoic tectonic elements in Central and Southeast European Alpine mountain belts: review and synthesis. Tectonophysics 352, 87–103.

Niu, Y., 2004. Bulk-rock major and trace element compositions of abyssal peridotites: implications for mantle melting, melt extraction and post-melting processes beneath mid-ocean ridges. Journal of Petrology 45, 2423–2458.

Okay, A.I., Sahintürk, Ö., 1997. Geology of the Eastern Pontides. In: Robinson, A.G. (Ed.), Regional and Petroleum Geology of the Black Sea and Surrounding Region, AAPG Memoir, vol. 68, pp. 291–311.

Okay, A.I., Satir, M., Tüysüz, O., Akyüz, S., Chen, F., 2001. The tectonics of the Strandja Massif: late-Variscan and mid-Mesozoic deforrmation and metamorphism in the northern Aegean. International Journal of Earth Sciences (Geologische Rundschau) 90, 217–233.

Okrostsvaridze, A.V., Clarke, D., Reynolds, P., 2002. Sm–Nd, Rb–Sr and K–Ar isotope system and geochemistry and geochronology age of the pre-Alpine granitoids of Dzirula salient of the Caucasian median massif. Georgian Academy of Science A. Janelidze Geological Institute Proceedings, New Series, vol. 117, pp. 173–186.

Pallister, J.S., Stacey, J.S., Fischer, L.B., Premo, W.R., 1988. Precambrian ophiolites of Arabia: geologic settings, U–Pb geochronology, Pb-isotope characteristics, and implication for continental accretion. Precambrian Research 38, 1–54.

Savov, I., Ryan, J., Haydoutou, I., Schijf, 2001. Late Precambrian Balkan-Carpathian ophiolite — a slice of the Pan-African ocean crust? Geochemical and tectonic insights from the Tcherni Vrach and Deli Jovan massif, Bulgaria and Serbia. Journal of Volcanology and Geothermal Research 110, 299–318.

Sengör, A.M.C., Natal'in, B.A., 1996. Palaeotectonics of Asia: fragments of a synthesis. In: Yin, A., Harrison, M. (Eds.), Tectonic Evolution of Asia. Cambridge University Press, Cambridge, England, pp. 486–640.

Shavishvili, I.D., 1983. Variscan volcanism in the Caucasus. In: Sassi, Szederkneyi (Eds.), IGCP 5, Newsletter, vol. 5, pp. 169–179.

Shengelia, D.M., Okrostsvaridze, A.V., 1998. New data on a structure of Dzirula salient of pre-Alpine basement of Georgian block. Dokladi Akademii Nauk 359, 801–803.

Shengelia, D.M., Vashakidze, V.T., Poporadze, H.G., 1988. The new data regarded metamorphics of Lokhi crystalline salient of the Transcaucasian median massif. Dokladi Akademii Nauk SSSR 30, 694–698.

Somin, M.L., 1991. Geological characteristics of the metamorphic complexes of the Great Caucasus. In: Korikovsky, S.P. (Ed.), The Petrology of Metamorphic Complexes of the Great Caucasus. Nauka, Moscow, pp. 8–43.

Stacey, J.S., Hedge, C.E., 1984. Geochronologic and isotopic evidence for Early Proterozoic crust in the eastern Arabian Shield. Geology 12, 310–313.

Stern, R.J., 1994. Arc assembly and continental collision in the Neoproterozoic East Africal Orogen: implications for the consolidation of Gondwanaland. In: Wetherill, G.W., Albee, A.L., Burke, K.C. (Eds.), Annual Review of Earth and Planetary Sciences, vol. 22, pp. 319–351.

Stern, R.J., 2004. Neoproterozoic ophiolites of the Arabian–Nubian Shield. In: Kusky, T.M. (Ed.), Precambrian Ophiolites and Related Rocks. Developments in Precambrian Geology, vol. 13. Elsevier, pp. 73–93.

Stern, R.J., Hedge, C.E., 1985. Geochronologic and isotopic constraints on late Precambrian crustal evolution in the Eastern Desert of Egypt. American Journal of Science 285, 97–127.

Stoeser, D.B., Camp, V.E., 1985. Pan-African microplate accretion of the Arabian Shield. Geological Society of America Bulletin 96, 817–826.

Sultan, M., Chamberlain, K.R., Bowring, S.A., Arvidson, R.E., 1990. Geochronologic and isotopic evidence for involvement of pre-Pan-African crust in the Nubian shield, Egypt. Geology 18, 761–764.

Sultan, M., Bickford, M.E., El Kaliouby, B., Arvidson, R.E., 1992. Common Pb systematics of Precambrian granitic rocks of the Nubian Shield and tectonic implications. Geological Society of America Bulletin 104, 456–470.

Sun, S.S., McDonough, W.F., 1989. Chemical and isotopic systematics of oceanic basalts: implications for mantle composition and process. Geological Society Special Publications, vol. 42, pp. 313–345.

Svanidze, Ts.I., Lobjanidze, Z.A., Jakobidze, E.B., 2000. Upper Triassic-Bajocian vegetation of the Western Georgia and stratigraphical significance of the flora. Geologica Balkanica 30 (1–2), 19–24.

Vail, J.R., 1985. Pan-African (late Precambrian) tectonic terrains and the reconstruction of the Arabian–Nubian Shield. Geology 13, 839–842.

Wasserburg, G.J., Jacobsen, S.B., DePaolo, D.J., McCulloch, M.T., Wen, T., 1981. Precise determination of Sm/Nd ratios: Sm and Nd isotopic abundances in standard solutions. Geochimica et Cosmochimica Acta 45, 2311–2323.

Wendt, I., Carl, C., 1991. The statistical distribution of the mean squared weighted deviation. Chemical Geology 86, 275–285.

White, W.M., Dupre, B., 1986. Sediment subduction and magma genesis in the Lesser Antilles: isotopic and trace element constraints. Journal of Geophysical Research 91, 5927–5941.

Yigitbas, E., Kerrich, R., Yilmaz, Y., Elmas, A., Xie, Q., 2002. Characteristics and geochemistry of Precambrian ophiolites and related volcanic rocks from the Istanbul–Zonguldak Unit, Northwestern Anatolia, Turkey: following the missing chain of the Precambrian South European suture zone to the east. Precambrian Research 132, 179–206.

Yilmaz, Y., Tüysüz, O., Yigitbas, E., Genç, S.C., Sengör, A.M.C., 1997. Geology and tectonic evolution of the Pontides. In: Robinson, A.G. (Ed.), Regional and Petroleum Geology of the Black Sea and Surrounding Region, AAPG Memoir, vol. 68, pp. 183–226.

Zagorchev, I., 2000. Rhodope and Vardar: the metamorphic and the olistromic paired belts related to the Cretaceous subduction under Europe. Comment: Rhodope facts and Tethys self-delusions. Geodynamica Acta 1, 55–59.

Zakariadze, G.S., Karpenko, S.F., Bazylev, B.A., Adamia, Sh.A., Oberhaensli, R.E., et al., 1998. Petrology, geochemistry, and Sm–Nd age of the pre-late Hercynian paleooceanic complex of the Dzirula salient, Transcaucasian massif. Petrology 6, 388–408 (Translated from Petrologiya, 1998, v. 6, No. 4, 422–444).

Zakariadze, G.S., Dilek, Y., Bogdanovsky, O.G., Karpenko, S.F., Vishnevskaya, V.S., Solov'eva, N.V., 2005. Age limits of the Lesser Caucasus paleo-oceanic allochthon. Abstracts of the International Symposium on the Geodynamics of Eastern Mediterranean: Active Tectonics of the Aegean Region, 15–18 June 2005, Kadir Has University, Istanbul, Turkey, p. 229.